WouldWood

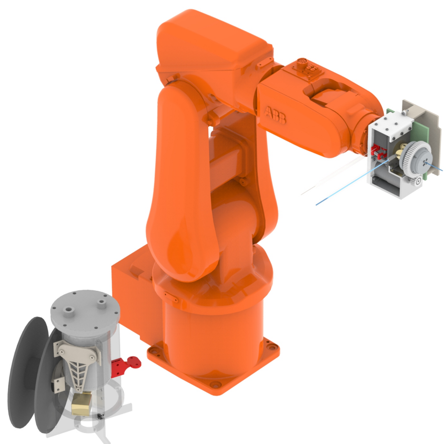

MF2059 Mechatronics Advanced Course

Erik Landman
941227-2735
elandman@kth.se

Erik Wedin
940620-6293
erikwed@kth.se

Kayan Phuong
940630-4585
kayanp@kth.se

Philip Pulli
940131-0173
ppulli@kth.se

Simon Ahlin Högfeldt
921012-3734
simonhog@kth.se

Simon Gärtner
900530-0950
sgartner@kth.se

Sourjya Chowdhury
931214-8613
sourjya@kth.se

Tobias Nilsson
940617-0499
tobinils@kth.se

Todd Barker
940906-9656
barker@kth.se

December 22, 2017

1 Abstract

This project explored the possibility of 3-D printing spatially, where the printed material consisted of at least 50 percent wooden fibers. The goal was constructing a modular printer that could print robust and environmentally friendly prototypes. The project was sponsored by KTH and Innventia, a leading Swedish wood-material research institute. Different methods of spatial printing were examined and a possible design based on requirements from Innventia were created. The design included coating the wooden fiber with UV-hardening resin and using a robot arm from ABB on which the printer head would be mounted. The design was split into different subsystems and a prototype was built. The prototype consisted of a modular printer head, feeding mechanism, pump system, UV - hardening system, cutting mechanism and the robot arm. UV - LEDs were integrated as a part of the hardening system in order to harden the resin coating. The overall system was made independent by implementing I/O communication between the subsystems and the robot.

The result showed that PLA resin effectively can coat and harden wooden fiber within a short period of time. The thread can become stiff enough to stay fixed in order to create different shapes.

This project is a continuation of the *TreeD* project from 2016. It was carried out by 9 Mechatronic students at the *Department of Mechatronics* at the *Royal Institute of Technology* in Stockholm, Sweden during the spring and fall of 2017.

2 Acknowledgement

During this project we have received invaluable help without which we would not have been able to finish the project. Among all the professional persons we have met during the project there are some we would like to acknowledge.

Firstly, we would like to thank Björn Möller and Andrii Berezovyskyi who have supervised and coached us throughout the course. Thank you for your time and support.

Furthermore, we would like to thank Staffan Qvarnström and Tomas Östberg for sharing their experience and providing a helping hand in constructional work. We would also like to thank Henrik Pettersson at Innventia for his help with testing and research.

Last but not the least, thanks to our friends in the Mechatronics Advanced Course for the many laughs and breaks. Especially Martin Åkerblad and William Bruce, for a much appreciated peer review of this report.

Last but far from least, Vicki Derbyshire. Thank you for making the entire institution go round.

Contents

List of Figures

List of Tables

3 Introduction

This report covers the design, manufacturing and implementation of a printer head prototype for printing cellulose-based thread spatially with the use of a robotic arm. This section describes the background of the project and covers state of the art in additive manufacturing, more specifically free-form spatial printing and the usage of cellulose-based materials.

3.1 Project Background

3-D printing or Additive Manufacturing (AM) techniques use different materials such as liquid, solid and powder polymers (powder metals and ceramics). The major advantages of using AM techniques include time and cost reduction along with the possibility to create complex shapes which otherwise would be difficult to machine.

According to an estimation done by Canalys in its recently released 3-D printing market study [2], accelerating technological development will drive the 3-D printing market value from its current 3.8 billion USD to 16.2 billion USD by 2018.

Plastics are the dominant 3-D printing materials today. According to SmarTech Markets Publishing report [3], 3-D printing is expected to generate 1.4 billion USD in plastics sales by 2019. In order to reduce this cost, the industry is experimenting with new material approaches, such as bio-based resins made from corn and soybean oil. Their applications can be found in various industries like packaging, automotive, construction, etc.

Unfortunately, there are several environmental issues related to the usage of plastics. According to Eriksen et al., [4] in 2014, it was estimated that 5.25 trillion plastic particles weighing 268,940 tons were floating in the sea. Plastic pollution is a substantial threat to the world today that has to be dealt with.

A solution could be the usage of bio-degradable plastics, derived from starch-based tubers such as sugar cane, corn, etc. The concept can be extended to the prospect of using wood in additive manufacturing and is currently a hot topic at Sweden's leading wood material research institute, Innventia. There is a strong incentive due to the fact that Sweden has a large wood industry and constitutes one of the world's leading exporters of paper, pulp and timber [5].

This project, WouldWood, is a collaboration between KTH and Innventia. The goal is to 3-D print spatially with a coated wood fiber. The project works towards merging technology within the fields of sustainable wood-based composites, advanced robotics and additive manufacturing in order to act as a proof of concept for future applications in construction work and architectural design.

3.2 TreeD

This is a continuation of a project named *TreeD*, conducted in 2016 by KTH students as part of a higher course in Mechatronics under the Engineering Design Masters track. The project resulted in a functional prototype for 3-D printing layer by layer, utilizing a PLA-coated cellulose fiber thread. The project used a Makergear M2 printer that was modified to use the developed extruder head that combined a wooden thread with PLA. The PLA and wood filament were bonded together by melting the PLA, adding wood filament and then cooling the mixture. The printer used g-code that was manually programmed for the printer to know what paths to take. Due to that the wood filament being used is a continuous thread, the user had to cut the thread manually when the print was done.

The aim of this project was to further develop the 3-D printing concept of utilizing cellulose mixture filament in conjunction with free-form spatial extrusion. This means that the printer head should not be used in a stationary 3-D printer, but should be mounted on a robotic arm. This would lead to possibilities in regards of spacial printing and not having to print using the layer by layer method used in the TreeD project.

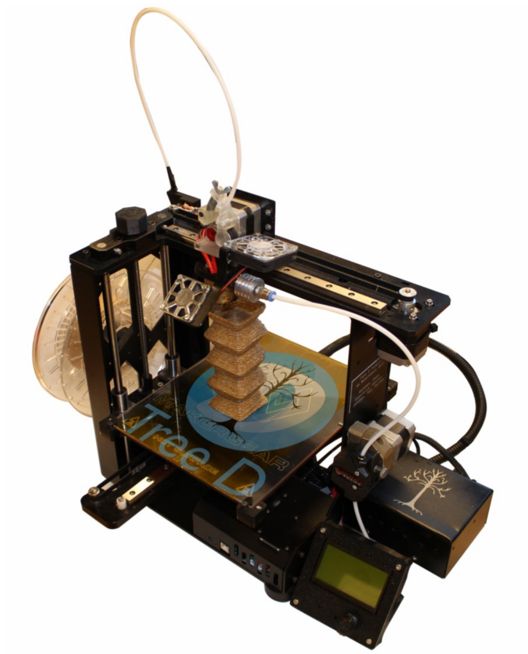

Figure 1: The 3D printer made by the previous project group. It is a modified 3D printer that uses a cellulose based yarn combined with PLA to print wooden structures.

3.3 Existing projects

Spatial 3-D printing is currently being investigated by multiple research projects. In parallel there is also research in progress with wood-based materials. A few interesting projects in the field of spacial 3-D printing and wood filament are mentioned below.

Mesh Mould, ETH Zurich

Using pin-point cooling, a research team from ETH in Zürich managed to build a mesh grid shown in Figure 2a. The team mounted an extrusion head on a 6DOF robot and created a mesh grid by using 3-D printing technique. The idea was using spatial 3-D printing technology to create complex, curved forms (mesh grids) used for example during the building process of concrete houses. Usually the mesh grid forms are responsible for a major part of the total construction cost. This was an incentive for finding another approach to building mesh grids. [6].

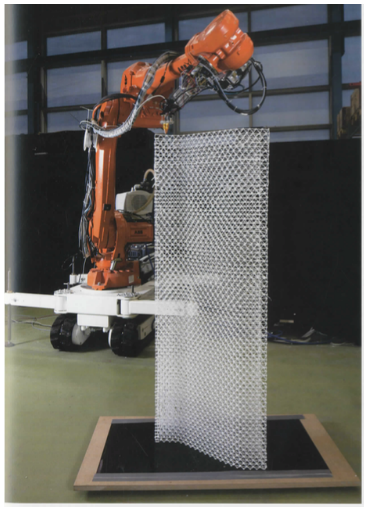

(a) ABB robot performing spatial extrusion

(b) Leaking Formwork

Figure 2: Project Mesh Mould, ETH Zurich.

Mesh Mould Metal ETH Zurich (2014-2017)

The Mesh Mould Metal -project was a continuation of the mesh mould project explained above. The goal was making the mesh structure more robust. By using 3 mm metal wire and automating cutting & welding with the help of a robot, they managed constructing complex structures in metal [7], see Figure 3.

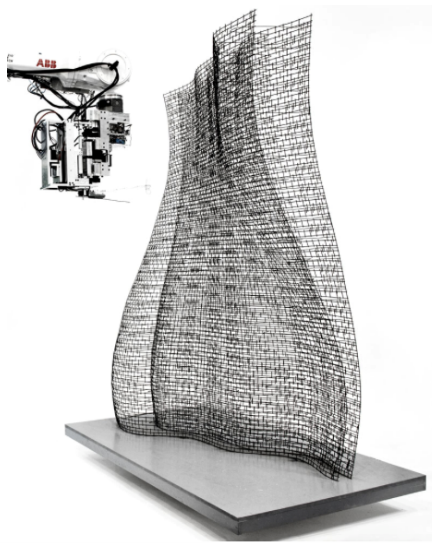

Figure 3: Mesh Mould in metal

Z - Unlimited

This project used an existing PLA printer and rotated it 180 degrees vertically. The printer was attached to a rail on the wall which let the PLA printer move freely upwards along the rail. This way they could print to a theoretically unlimited height, as depicted in Figure 4. One advantage of this concept is that the design uses a slightly modified existing technology which reduces development cost. The modification package costs between €400 to €700. Furthermore the product is robust and easy to use. [8].

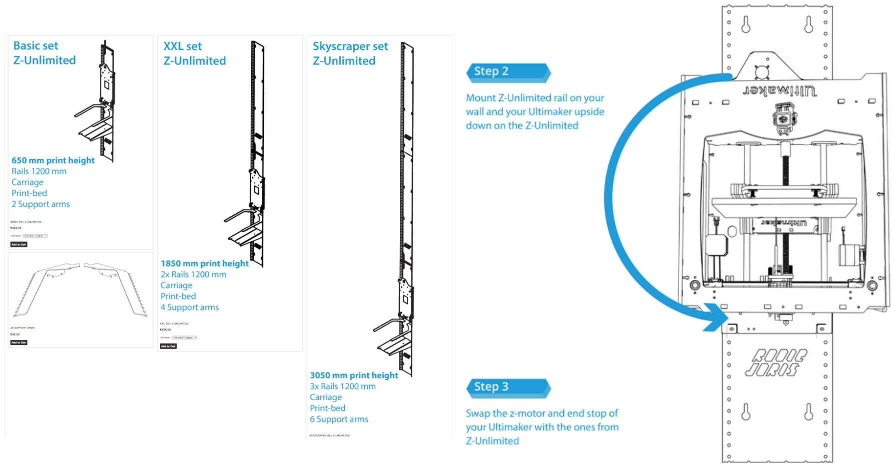

Figure 4: Z print

Apis-cor 3-D printing a house

A rotating 3-D printer is placed in the center of the house. The arm can rotate and prints the house with a fiber concrete or geopolymer. The printer prints layer-by-layer but can print out of the box. The printer can do internal and external walls of buildings and other vertical fencing structures, permanent foundation formwork, precast-monolithic slabs, as well as a variety of structures and small architectural forms, such as columns. Printing the parts of the house seen in in Figure 5 took 24 hours [9].

Figure 5: Apis-cor 3-D printed house. The complete print took 24 hours to complete.

Mataerial

This 3-D printer from the Institute of Advanced Architecture of Catalonia uses thermosetting polymers as printing material. A chemical reaction between two chemical components of the extruded mixture in addition to heating the material with two heat blowers directly after extrusion causes the material to solidify very rapidly. This way suspended beams of any shape can be created without the need of support structure. The system prints at the rate of 1 m in roughly 3 min and the printed beam is estimated to be thicker than 5 mm [10]. The machine does not use any wood fibers. Figure 6 shows the printer and a close up of the printer head.

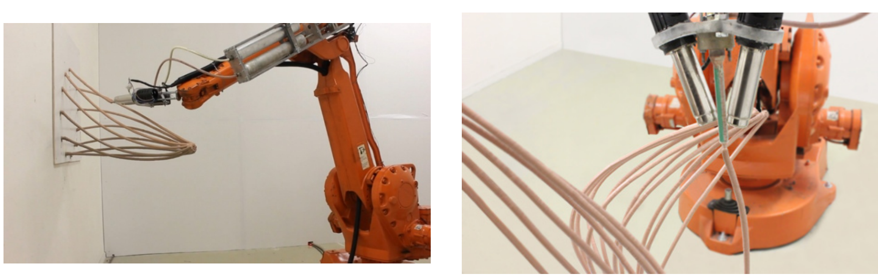

Figure 6: (Left) Mataerial printing suspended beams, (Right) close-up of the printer head

Atropos

Atropos uses an acrylate based UV-set mixed with fibers. Currently glass and basalt fibers are being used, but work is done to make mixtures with carbon, polyaramides and bamboo fibers. The alignment of the fibers gives the material high strength in the longitudinal direction, allowing for making structures specifically designed for the load direction. The mixture is transported to the printer head which is mounted on a robotic arm. The printer head has two UV-light sources on the side, which induces polymerization of the material after extrusion. The printer is able to print at speeds of 2.5 cm/s [11].

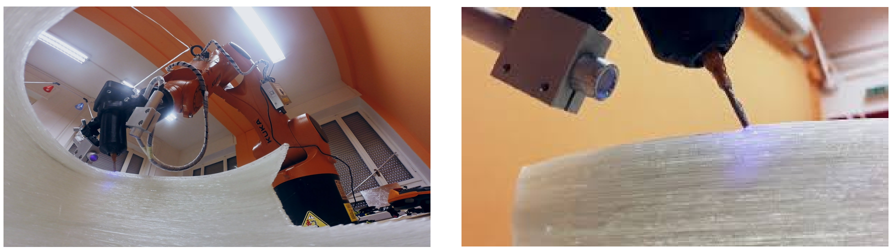

Figure 7: (Left) Atropos printing 3-D structure (Right) close-up of the printer head

3.4 Material

PLA

PLA (short for polylactic acid) is a thermoplastic polymer that is produced by fermenting and polymerizing naturally occurring raw materials (sugarcane for example). In the year of 2016, PLA constituted 5.1% of the globally produced bioplastic making it the second most common of all biodegradable plastics [12].

Although bio-plastics are mainly used for packaging, it is needless to say that PLA in particular plays a huge role in 3-D printing, competing only with ABS-plastic in terms of convention. Whichever choice is preferable depends on the application, but in any case the list of desirable attributes of PLA is long; low warping, molten viscosity and melting temperature for the sake of naming a few [13].

Within the scope of WouldWood the main reasons why PLA is an attractive alternative are:

- The prototype handed down from last year's team offers an already existing solution for coating cellulose yarn with PLA.
- There lies a strong environmental incentive in using PLA since it would yield a composite which is fully bio-based.
- Widely used as it is, the sheer amount of easily available information

makes PLA appealing.

However, remaining within the scope of WouldWood and more specifically the end goal of the project, there are also downsides to using PLA. Early phase testing (not included in this report) unraveled that spatial printing (as opposed to printing layer-by-layer) with molten thermoplastic requires a far more sophisticated cooling system than the one currently available, due to the print sagging without the presence of an already stiffened support structure. Although the mesh-mould project mentioned previously in section 3.3 Existing projects successfully overcame the challenges of rapid cooling there are cases where said challenge has been avoided by using fundamentally different materials such as the Mataerial and Atropos projects mentioned in section 3.3 Existing projects.

Thermosets

In contrast to thermoplastics, thermosetting polymers do not soften or liquify when heated. Thermosetting polymers form cross-links between molecular chains during curing, making them permanently hard. Thermosetting polymers are therefore generally stronger and harder than thermoplastics such as PLA [14]. Curing can be done by applying heat, radiation or mixing with a catalyst.

Stereolithography

Thermosetting resins are already being used in 3-D printers based on stereolithography. In stereolithography a thin layer of liquid resin is deposited on the building platform. Using a laser beam the pattern that needs to be solidified is drawn on the liquid which is cured by the laser. The partially printed object is then lifted up by the thickness of one layer and this cycle is repeated for each layer [15]. Because the accuracy of the stereolithography printers is mostly dependent on how accurately the laser beam can be focused, higher accuracies can generally be obtained than with printers based on fused-deposition modeling using thermoplastics.

Fiber reinforced polymer composites

Adding fibers to the filament in order to improve the mechanical properties of the printed structures has been shown in literature by several groups ([16], [17], [18]).

One example used a mixture of a photo curable acrylate with a heat curable epoxy and added 5 wt. % of carbon- or glass fiber [16]. The acrylate cured under UV-light during printing, quickly hardening the material after deposition. Then the object got a heating treatment, curing the epoxy improving the mechanical properties of the material. The elastic modulus of the cured material without fibers was 2.7 GPa with a maximum strength of 16 MPa. This increased to 4.4 GPa and 33.8 MPa respectively when carbon fibers were added. Using this mixture they managed to print overhangs up to 30° at a speed of 10 mm/s and a UV exposure time of 30 min.
Another group managed to get better mechanical properties using an epoxy

based filament with 17.4 vol. % silicon carbide whisker and carbon fibers [18]. The fibers align in the printer head, because of its small diameter. They obtained an elastic modulus of 6.2 GPa and a maximum strength of 29.2 MPa for the material without fibers. For the material with the fibers this increased to an elastic modulus of 24.5 GPa and a maximum strength of 66 MPa in the direction of the fibers. Strength in the transverse was less drastically improved to 8.1 GPa and 43.9 MPa.

4 Design considerations

During the design process, there are several aspects that should be taken into consideration in order to develop a functioning product that satisfies its user's needs. In this chapter, the requirements and limitations of this project will be discussed.

4.1 Requirements

Since this project was a collaboration between KTH and Innventia, they had requirements for the complete construction. These requirements are defined as stakeholder requirements and describe the main goals as well as general outcome of the project. Using these, the project team decided user requirements that further help defining the essential functions of the construction of the printer. In the end, technical requirements were specified. They help quantifying crucial aspects of the construction. The user requirements as well as the technical requirements has been developed during the timeframe of the project. The major requirements are given below as a simplified summary.

Stakeholder Requirements
The stakeholder requirements has been developed by discussions with the stakeholders KTH and Innventia. During this process, limitations and the scope of the project was decided.

1. The printer shall print without using a layer-by-layer method.
2. The printer shall print using no less than 50 % cellulose fibers.
3. The printer shall not use support structures for printing objects.
4. The printer shall not produce toxic fumes that can affect the user's health.
5. The wood filament shall be cut when needed.
6. The printer head shall be modular.

User Requirements
A variety of user requirements were developed by the group after the discussions with the stakeholders were complete. The user requirements has been developed with functionality in mind. It was decided to use a robot arm since it is a robust way to have easily attach a modular printer head. This would give the benefit of having the printer being able to move freely in the three dimensional space, but with some limitations. In order to print objects, there has to be a high accuracy of the position of the printer head. The thread has to be properly coated, so it will not bend when printed. Furthermore, it has to be able to withstand being fed at various speeds since the coating could harden at different speed. The coated thread must be able to be cut off so that the printed structure can be removed. The user requirements for the project is given below.

1. The printer head shall be mounted on a robotic arm.
2. The printer head shall be positioned with high accuracy.
3. The thread shall be evenly coated with coating material.
4. The thread shall be fed with high repeatability at various speeds.
5. The coated thread shall harden quickly.
6. The thread shall be cut with a high repeatability.

Technical Requirements

The technical requirements were chosen based on measurable parameters. For example, the robot IRB120 has a given limit to the payload it can handle. The thread has to be positioned with a margin that was estimated to $\pm$ 10 %. Furthermore, it was estimated that the thread had to be fed at a speed interval between 0-5 mm/s. That was based on quick tests of how quick the coating material hardened.

1. The total weight of the printer head shall not exceed 3 kg.
2. The repeatability of the nozzle position in the robots workspace shall be less than 10 % of the nozzle diameter.
3. The thread shall be fed within the speed interval 0-5 mm/s
4. The printer shall have an emergency stop.

Subsystems

During the development of the various requirements, the project was divided into smaller subsystems. These parts were developed with modularity in mind, being able to be set together as a complete modular system.

1. Robot - The controlling of the robot as well as mounting of the printer head.
2. Material - The material used for printing in regards of wood filament and resin.
3. Printer head - The complete printer head containing different modules.
4. Thread feeding - The system for feeding the thread.
5. Coater - The part of the printer head that coats the fed thread with the chosen resin.
6. Resin feeding - Depending on the chosen resin, it has to be fed to the printer head.
7. Cutter - The system that will cut the thread when needed.
8. Curing - Depending on the resin used, it has to be cured in some way.
9. Controller - The communication system between the different parts of the complete product and robot.

4.2 Robot

Following the user requirements, a robotic arm was to be used to mount the printer head. The main idea was that the robotic arm would be programmed to do the wanted movement for the print while communicating with an MCU that would control the tasks needed for printing. Using a robotic arm for printing would allow for spacial printing and a wide range of motion. For example, the robotic arm can rotate its arm 180° and therefore print downwards.

During the beginning of the project, using an IRB 14000 which is also known as YuMi, was considered. Because the YuMi has a Profibus port and using a Profibus would simplify implementing the communication between the robot and the printer head MCU, the decision to use a Profibus was made. However, due to availability issues, a YuMi could not be used.

An IRB 120 robot from ABB [19] was therefore used instead. The IRB 120 was considered suitable due to its relatively small size, its great movement flexibility, path accuracy and load capacity. Additionally the construction of the head of the robot simplified attaching an external device. The robot is connected to an IRC5 M2004 controller [20]. This controller does not use Profibus and therefore a change of plans revolving the communication had to be made. The controller uses a standard COM port as well as I/O pins. Therefore, a combination of those two were of consideration for the communication.

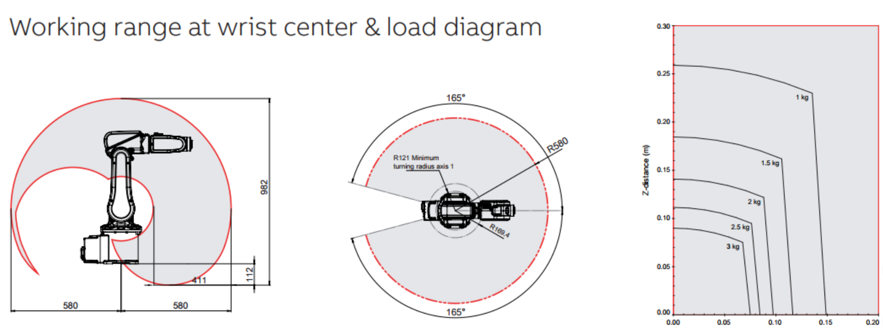

Figure 8: Working range of the IRB 120 Robot

Axis Movements	Working Range	Maximum Speed
Axis 1 Rotation	$165°$ to $-165°$	250 °/s
Axis 2 Arm	$110°$ to $-110°$	250 °/s
Axis 3 Arm	$70°$ to $-110°$	250 °/s
Axis 4 Wrist	$160°$ to $-160°$	320 °/s
Axis 5 Bend	$120°$ to $-120°$	320 °/s
Axis 6 Rotation	$400°$ to $-400°$	420 °/s

Table 1: The working range and maximum speed of the different axis of the robot.

4.3 Material

Free-form printing in space demands a better coating material than the PLA that was used by the TreeD-team. Initial tests were conducted with the handed down equipment from last year, concluding that the task of cooling PLA fast enough to a temperature at which it is stiff enough to prevent sagging of a just printed segment is challenging to say the least. There was a strong incentive for trying a new approach.

It was decided to use a resin that is curable with UV-light, as UV-curable resin can be cured quickly with a focused beam of UV-light on the thread. For the choice of which UV-set to use, the resin used in Formlabs SLA-printers was compared to samples from chemical specialist companies.

Testing was conducted by dipping a piece of thread in resin and subsequently curing it with a Coolled pE-100 with a 3 mm-thick lightguide. The Formlabs resin cured within a few seconds to a sufficiently stiff state, while the other resins stayed sticky and flexible in comparison. Because the Formlabs resin was easily available and cheaper than the explored alternatives, it was chosen for this project.

4.4 Printer Head

In this project, the part called 'Printer Head' refers to the entire construction that is mounted on the robot arm. The different parts will be discussed in later chapters.

The printer head will need to have a frame to keep the different components together. Furthermore, it has to be attachable to the the robot arm. The size and weight of the components will determine the form and structure of the frame. It is important to bear in mind that the printer head will be mounted onto the *6th* axis(rotational) of the robot. The *5th* axis is the bending axis. The width of the printer head is constrained to make sure that once the *5th* axis is bent at its maximum angle of 120°, the printer head will not collide with the robot arm.

As mentioned in section 4.1 Requirements the printer head shall be modular meaning it ought to be easy to mount it onto the robot. However, the system needs to be small enough to avoid collision with the arm itself and the 3D printed objects, which might affect the modularity and the assembling process.

The weight of the printer head shall not exceed the IRB120's payload which is 3 kg. This includes the wires and tubes that will be connected to the printer head. Therefore, the frame and mount will be manufactured in a light material.

4.5 Thread feeding

In the previous project TreeD, the feeding was done by having two rotating wheels feeding the thread. One of the wheels was mounted on a stepper motor and the other wheel could rotate freely. The wheels were pressed together with a spring with the thread in between them.

During the current project, a variety of tests were conducted with the *TreeD* printer in order to see the problems for the current feeder as well as the improvements that could be made. These tests showed that the wheels had problems gripping the thread, i.e. the wheels would rotate but the thread would not always move. When designing the feeding mechanism, this problem had to be dealt with. One conclusion of the tests was that the friction between the two wheels was important for the gripping aspect. The friction could be increased by selecting a more suitable material. For example by adding sandpaper or rubber to one or both of the wheels. The *TreeD* project used rubber on one wheel and sandpaper on the other. There was also a small trace in the rubber in order to keep the thread in the middle of the wheels. However, this also reduced the grip, which subsequently led to slipping of the thread.

Another issue that has to be taken into consideration is the flexibility of the thread. Because the thread is flexible there was a risk that the tread might curl when pushed forward. For reducing the risk of thread curling, the feeding mechanism had to be placed as close to the extruder as possible. Additionally, the thread should be guided by a channel, which is small enough that the thread will not curl inside it, but not so small that it cannot move easily through the channel, since that would cause the thread to curl.

4.6 Coating

Coating the thread is an essential aspect of the printer head functionality; regardless of the substance at hand (be it molten PLA or UV-setting resin) an evenly distributed *stiff* layer is key to maintaining any kind of structure and print-quality.

Available at the very beginning of the project was an existing coater handed down from last years project. It was established at an early phase that the design and manufacturing of a superior coater was unrealistic within the limits of this years time-frame and desired outcomes. In consequence, the given coater was kept, slightly altered and used as a design interface for other subsystems.

4.7 Resin feeding

The resin constitutes a vital part of the compound to be fed to the nozzle and the ability to move it in controlled amounts at specific times is a crucial aspect of the design. This warrants a subsystem capable of both feeding resin and sensing how much is being fed through the system.

Overview
The system is demanded to fulfill a certain set of requirements. These include consistent flow independent of printer head position, the capability of feeding a viscous liquid of 800 cps, UV blocking to prevent unintentional hardening of resin and finally a tolerable practice of managing a toxic substance. In addition the flow rate provided by the system is required to match assumed print speeds of 5 mm/s to 10 mm/s, which in combination with the requirement that the volume ratio between wood and plastic has to be 50 % yields the following required flow rate:

$$Q_{resin} = \frac{\pi r^2 v_{thread}}{2}, \tag{1}$$

where r is the radius of nozzle outlet and v_{thread} is the velocity of the thread at the current print speed. This gave the flow value of 49.1 µl/s to 98.2 µl/s. Furthermore, it is preferred that the system runs on 24 VDC or less due to the available power supplies.

Actuation
There are three commonly applied ways to move a liquid in a controlled manor; a pump, a pressurized system with a controllable valve and lastly utilizing gravity. These are all looked into below.

Gravity
The gravity principle is commonly used in water supply for cities, e.g water towers, and is based on a reservoir placed on a higher level than the outlet, resulting in a pressure difference between the reservoir and the outlet meaning the fluid is pushed out of the outlet once it opens. This method is inflexible and the outlet flow will be dependent on several uncontrollable variables such as the hight of the reservoir, how much fluids is left in the reservoir and the position of the outlet.

Pump
The concept of a pump has been around for thousands of years starting with man powered screws and arm actuated pumps to electrical pumps for industrial use down to nano precision in medical use, suggesting that manufacturers might be able provide a pump according to specification. For this consideration two manufacturers, Micropump and Telfa, were contacted and discussion with their expert was conducted on what would possibly suit the given system and requirements.

Pressure
The pressure chamber is based on the same principle as the gravity system meaning it too creates a pressure difference between the two ends of the system, only here the difference comes from induced pressure and not gravity. This is achieved through a pump that adds air to a enclosed chamber with a valve on the outlet. This means that one can obtain a fully controllable system in terms of flow and the pump only has to move air.

Concept
The latter concept was evaluated by replicating the real system and performing tests. The setup which was comprised of an air pump, a solenoid valve and a PET-bottle, is shown in figure 9 below:

Figure 9: Test Rig of Resin Feeding

The test was conducted using an analog for the resin, syrup, to match viscosity and stickiness [21]. No legitimate measurements were taken due to lack of necessary equipment. Instead the test was seen as a proof of concept and a successful one.

Sensing
Controlled feeding demands closed loop feedback from the outlet. For the sensing aspect of the resin feeding system two methods were considered, flow and pressure sensing. In addition to the previously mentioned requirements concerning resin feeding, sensor outputs should preferably be readable by the chosen MCU and also not take up to much processing power, as might be the case for an interrupt-driven sensor technique.

Flow meter
A flow meter does what the name implies, measures flow. It is put in series with the flow of fluid, causing a wheel inside the sensor to turn. The rotation of the wheel is carefully measured with an encoder which combined with the knowledge of the cross section area gives highly accurate measurements of the flow. Within the context there are however two major drawbacks; when designed for low flows the sensors become small and sensitive, making them *expensive* and *vulnerable* to a fluid with properties like the resin.

Pressure
The pressure sensor is measuring pressure through a membrane that measures the force of the fluid or air that acts upon it and by knowing the membrane area

the pressure can be calculated. A pressure sensor would be installed in parallel to the flow before and after the actuation of the feeding. This way the pressure alone on the outlet or the difference between the two can give a measurement of how much flow the system experiences. This is a robust and cheap solution, however it needs a lot of calibration.

4.8 Cutter

Problem
For the same reasons an artist lifts his/her pen from a sheet of paper a free-form 3D-printer must be able to stop printing in one position and continue at another. In this case it is therefore necessary to be able to cut the otherwise continuous thread.

When considering the design and placement of a cutting mechanism one must take into account the control over the extrusion. Severing the thread inside the printer head (I.E. before the nozzle) poses a problem because of the loose and flexible end that would then need to be fed the distance between the cutter and the nozzle tip. Although the extent of this challenge depends on the capability of the feeding mechanism, it is clear that the thread would advantageously be cut as close to the nozzle as possible from a feedability standpoint. Yet another motive arises when considering the special case of printing segments shorter than the offset between nozzle and cutter, in which each cut would result in a loose piece of thread in the extrusion channel, reducing control over extrusion at best and creating the additional risk of clogging the printer head.

The need for placing the thread cutting mechanism at the tip of the printer head results in size restrictions on the design of the cutter. The cone angle of the nozzle (i.e. how pointy the nozzle is) determines the angle at which the printer head can be tilted without intersecting the plane it is printing in and hence the freedom of forming. It is therefore important that the size of the cutter is kept at a minimum.

Further, it is desirable that a cutting action is achieved without deforming the already printed line. This results in the need for a sharp edge and a design that holds the thread in place on cutting impact. Lastly, the cutting speed should preferably be high.

Concept
At an early stage there was a suggestion promoting a particular concept for cutting; due to the demands mentioned above and the circular geometry of the coater a rotational mechanism seemed appropriate. The principle is conveniently illustrated by figure 10, portraying a simple test-rig that was developed for verification of the mentioned concept: Having two surfaces mounted against

each other, with one off-centered hole going through each (one of which the inside is sharpened), feeding a piece of thread through the two holes and rotating one of the two surfaces, causing a dissection of the thread.

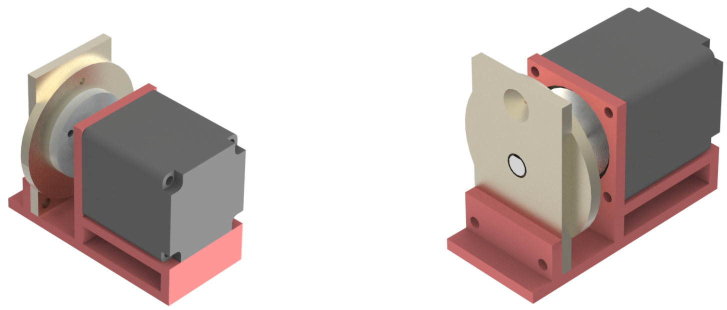

Figure 10: Concept for cutting - Test rig with stepper motor and disks

Outcome
The test-rig granted not only an assessment of the required sharpness; by making small alterations in the test-rig design and performing rapid prototyping a range of motors could be tested in pursuit of adequate cutting power. Tests showed that cutting through a cellulose based thread requires more than anticipated:

- There was an intention of using a stepper motor due to qualities such as precise positioning and ease in implementation. This was abandoned due to the insufficient torque provided and it was concluded that a high torque DC-motor with an encoder had to be used.

- It became clear that the required sharpness was not going to be reached by sharpening the inside of a hole. Somehow a proper blade had to be implemented.

4.9 Curing

Problem
For the sake of the ability to print more than straight lines it is essential for the design that curing takes place after the thread exits the nozzle; bending would not be possible if the thread was hardened before exiting. It is equally important that the coated thread is cured as close to the exit point as possible for minimizing the risk of sagging or otherwise deforming between the points of exiting and curing.

The speed of curing is a key factor for the printing speed and should therefore be as fast as possible. The curing speed can be increased by using a higher intensity light source, placing the light source closer to thread or by focusing the light more on the thread. Although the curing must take place after nozzle-exiting and the light source needs to be as close to thread as possible the source may not stick out below the nozzle as this would cause them to intersect the printing plane, negatively affecting the freedom of form.

Equipment
For UV-light sources, the previously mentioned Coolled pE-100, the BlueWave series from Dymax and a self-build system with 5 Vishay VLMU3500 UV-LEDs and a Recom RCD-24-0.70/W/X3 LED-driver were compared. The pE-100 and BlueWave series both work with a control box that contains the light source and one or multiple light guides, which are optical cables with a lense at the end for spot curing. The pE-100 has an intensity of 300 mW/mm^2, which has proven to be sufficient during the material tests, albeit not the fastest curing. The light sources in the BlueWave series have an intensity ranging from 90 mW/mm^2 to 400 mW/mm^2 and should thus be able to cure the coating. These can connect up to four lightguides to one source. The Coolled can only connect one led, so multiple sources or a mirror system would be needed to cure the thread on all sides.

The biggest disadvantage of both of these systems is their price, as they can easily cost 50 000 SEK. For this reason, it was first tested if sufficient results could be achieved using the significantly cheaper self-build solution. Five LEDs were soldered to individual PCBs, connected in series and mounted in the slots of the circular prototype shown below in figure 11, LEDs facing inward toward the concentric through-hole. Hardening scenarios were simulated by passing hand-coated thread through the hole whilst driving the LEDs at different intensities.

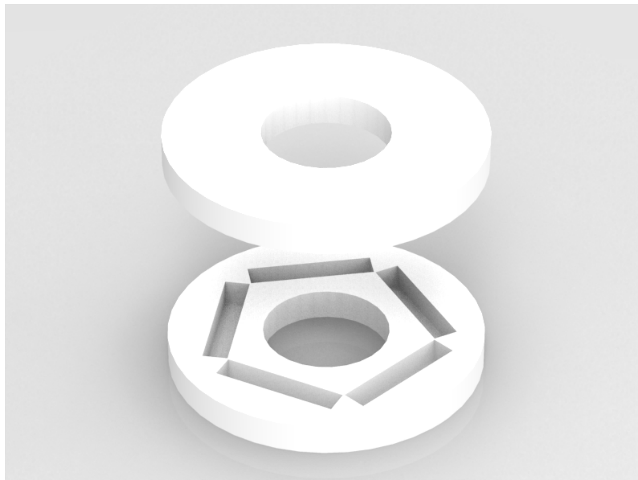

Figure 11: LED-holder

Outcome
The hardening speed and thread stiffness were deemed to be satisfactory. Each LED has an intensity of 1.25 W at maximum power, at which they developed extreme heat but curing was almost instant. At 20 % power the curing was sufficiently fast and heat was manageable.

Although the industrial solutions do not have heat issues and offer the convenience of spot curing with a light guide their price is too steep. A self-build curing system is chosen despite the fact that the printer might need pauses during operation to let the LEDs cool down.

4.10 Controller

Each identified subsystem has varying control needs, which are listed below. These are based on the user requirements, which can be found in section 4.1 Requirements.

Robot
As stated in the Requirements, the robot needs high precision in the positioning off the printer head nozzle and movement in 3D space. The robot uses a built in controller to achieve this. No extra control was deemed necessary. However, the timing between the robots movement and the printer head MCU sub functions needs to work synchronously in real-time. The synchronization was controlled using hardware timers on the printer head MCU and a series of interrupt exchanges between the Robot and MCU, which are described in greater detail in

sections 5.7 Software.

Curing process
The curing process, described in section 4.9 Curing, needs to be done rapidly to allow for greater feeding and printing speeds. The resin was cured using high intensity UV-LEDs. The LEDs needed a high current to function and were therefore controlled via a LED-driver. The LED-driver uses a PWM signal to control the intensity. Since initial tests showed that curing was almost instant for a high enough duty cycle, an open-loop system was deemed sufficient to control the curing process, meaning no controller design was performed.

Cutting
Because a high repeatability for the cutting of the thread was required, a certain torque and velocity needed to be reached in order to cut through the thread reliably. Therefore, a model of the cutter mechanism was developed (described in section **?? ??**) and control parameters were tested out in the simulation. The control parameters were then implemented and tuned, to catch any error in the model design.

Resin Feeding
The resin feeding should be controlled in such a way that when thread is being fed there is a constant flow of resin and no flow when no thread is being fed. The resin should be evenly distributed over the surface of the thread. It was found that in order to get an even layer of resin on the thread the pressure of the resin in the coater should be kept constant. A control loop is thus needed that regulates the pressure in the resin tank. Additionally, the control should be able to quickly start and stop the resin flow, by opening and closing the valve after receiving a control signal from the printer head MCU.
In order to find good control parameters the pump system was simulated and based on the results the controller was implemented. This is described in **?? ??**.

Thread Feeding
The requirements state that both the amount of thread that is fed as well as the speed at which the feeding is done should be controlled. Stepper motors give precise control over the amount of rotation and thus over the amount of thread that is fed. To control the speed of the feeding as well the step count should be increased at a precisely controlled rate.

5 Design implementation

This section discusses how the design implementation of the entire system is done to meet the requirements and specifications. First an overview is given of all the subsystem and how they fit together. Then the design of each subsystem is detailed.

5.1 System Overview

Figure 12 shows an overview of all the subsystem of the printer and the communication between them.

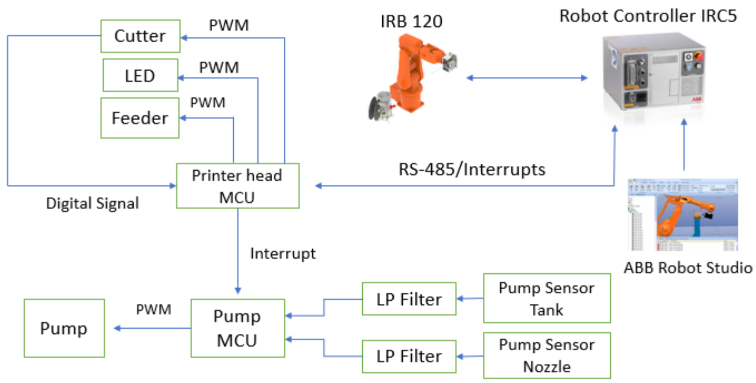

Figure 12: Overview of the complete system. The blue lines shows the communication between the various subsystems.

From the software called RobotStudio, code for the robot movement and communication is generated and then transfered to the IRC5 controller. The controller is connected to the robot and tells the robot when and where to move. The IRC5 controller is connected to an MCU on the printer head and instructs the MCU which and when an action is to be executed. The printer head MCU controls the feeding, curing and cutting and instructs the pump, according to the action currently being executed.

The communication between the MCU and IRC5 controller is done using serial communication to send which actions are to be executed next and using interrupts via I/O pins for the timing of when these actions are to be executed. The pump station is controlled by its own MCU, which receives instructions from the printer head MCU about when to pump up resin. Flow charts detailing how the communication between the robot and printer head MCU is executed can be seen in section 5.7 Software.

5.2 Robot

An IRB120 robot arm from ABB (figure 13) was used to mount the printer head on. The IRB120 uses an IRC5 M2004 controller (figure 14). The robot has several I/O pins connected via a D-sub connection, which is called XS-7 for this particular controller. The robot also uses a COM port for communication. In order to use the I/O pins from the controller, some modifications had to be made on the controller itself. The I/O pins need 24 V and a connection to ground to work. The controller had another D-sub connector called XS-6. On this connector, 24 V was available. Cables from 24 V and GND were therefore connected from XS-6 to XS-7 in order to provide it with the necessary voltages.

Figure 13: An IRB120 from ABB.

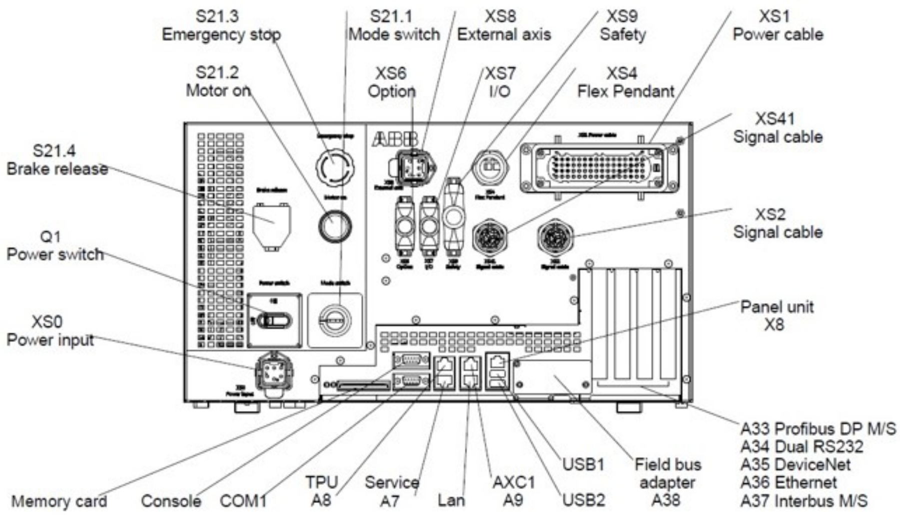

Figure 14: An ABB IRC5 controller.

The controller has in total 36 I/O pins on the XS-7 connector, which are divided into two sections. The I/O pins 1-16 are predefined as outputs while pins 17-36 are predefined as inputs.

For this project, three I/O pins were used. The controller used two input pins to receive interrupts from the printer head MCU. These were used to signal when the MCU was ready to receive and execute commands. One output from the controller was used. Its purpose was to signal the timing for starting and stopping the execution of a command.

5.3 Printer head

The entire system was modeled in the 3D CAD software Solid Edge ST 8. To ensure that the entire printer head was suitable for the IRB120 robot arm, the 3D model of IRB120 was downloaded in STL format. These files were converted to Solid Edge part files to be compatible with the printer head files.

The subsystems were modeled first, before the mount and the frame were created. The overall form of the printer head (figure 15) was designed to have a block form similar to the IRB120 robot arm.

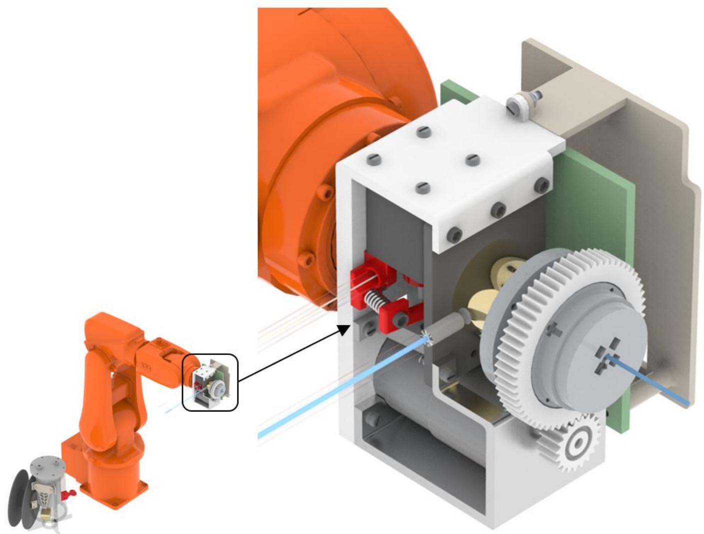

Figure 15: Overview of the printer head mounted onto the IRB120.

The measurements of the complete printer head are:

- Height: 101 mm [robot arm - tip of the printer head]
- Length: 130 mm [stepper motor - DC motor attachment]
- Width: 107 mm [PCB holder - thread/resin input]
- Weight: 860 g

A detailed view of the system can be seen seen in figure 16 where all the subsystems are pointed out. In the following, each subsystem will be described thoroughly.

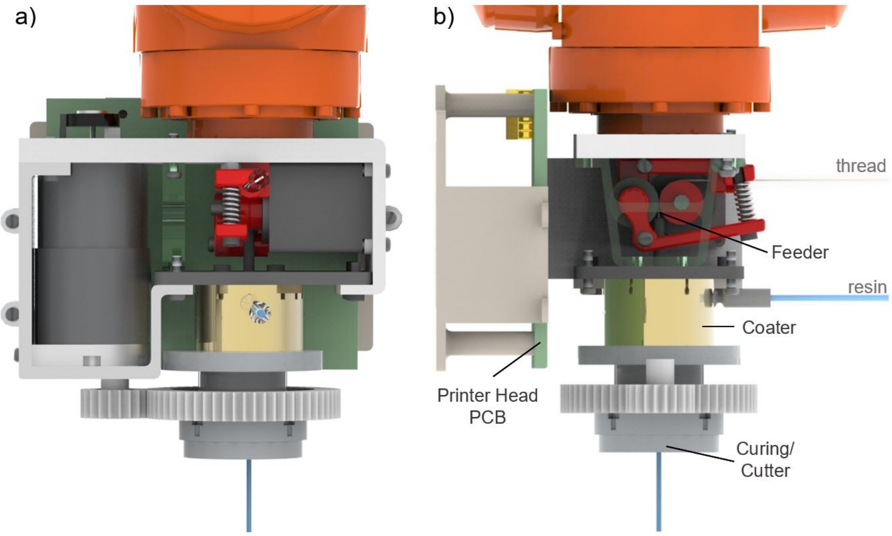

Figure 16: a) Side view of the printer head, b) Close-up of the inner components.

Frame

The subsystems are connected by a frame structure that consists of five parts (figure 17).

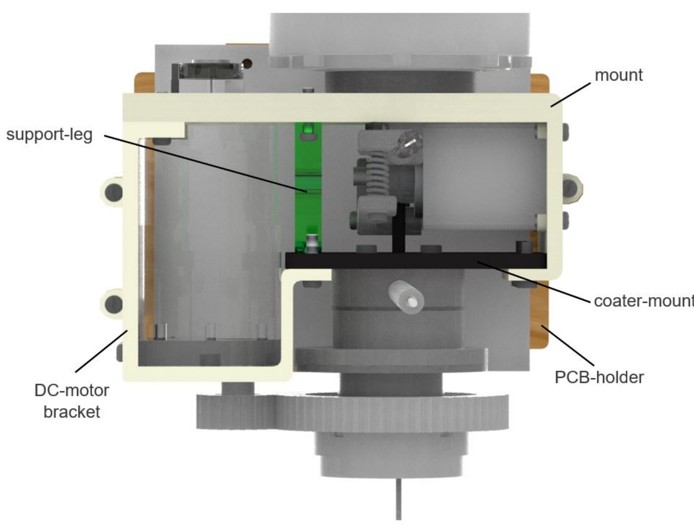

Figure 17: Frame structure of the printer head

Each part has its own purpose where the *mount* is used to attach the printer head onto the robot arm. The *mount* also functions as a holder for the feeding system. The coater is fixed to the mount with the help of the *coater mount*. The *DC-motor bracket* is also connected to the *mount* and supports the other end of the *coater-mount*. The relatively heavy weight of the coater and DC-motor might cause a non-steady frame structure or might even break the screw joints. A *support-leg* is therefore placed between the mount and coater mount to reinforce the joints. Lastly, the printer head PCB is attached to the printer head with the *PCB holder*. These parts were 3D printed with either an Ultimaker 2 or a Formlabs Form 2.

Thread feeding

The feeding mechanism that was used in ThreeD did work, but had some gripping issues. A similar design for the mechanism was made to suit this project (figure 18). The wheel on the *feeder arm* is pressed against the wheel driven by the *stepper motor* with a spring. One of the changes was redesigning the wheel holders, *feeding arm* and *feeding base*, to fit the chosen stepper motor. Furthermore, the rubber that covered one of the wheels was replaced with sandpaper, so that both wheels now have sandpaper and have better grip on the thread. The two wheels were 3D printed with an Ultimaker 2 and the feeding base and arm were printed with Formlabs Form 2 machines.

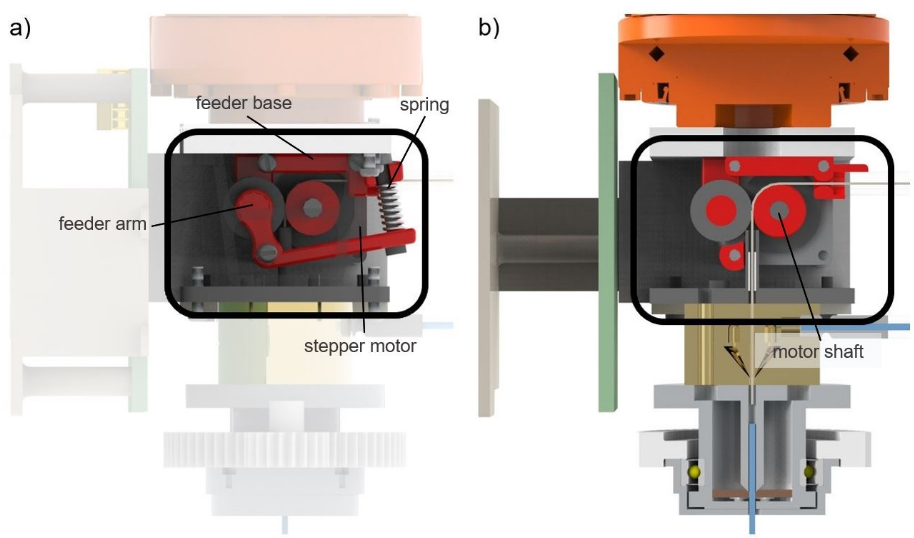

Figure 18: Feeder mechanism. a) Close-up on the feeder mechanism. b) Section-view of the mechanism.

As mentioned in section 4.5 Thread feeding, keeping the thread from curling during the feeding process is important. This problem was solved by creating guides in every part that the thread would pass by or go through. These paths are highlighted in figure 19.

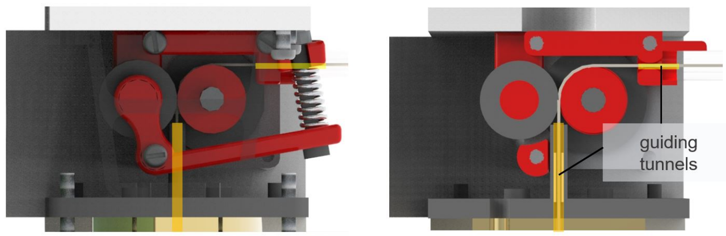

Figure 19: Highlighted guiding paths of the feeder system

The thread feed speed can be described as:

$$v_{thread} = \frac{s_{step}}{t_{step}}, \tag{2}$$

where t_{step} is the time between steps and s_{step} is the distance for each step, which can be calculated by following equation:

$$s_{step} = \frac{2\pi r}{N}, \tag{3}$$

where r is the radius of the feeding wheal and N is the amount of steps needed for one revolution. To change the speed, the variable t_{step} is changed to get the required speed necessary.

Coater

Once the thread is fed to the coater the thread goes through a small basin filled with resin which is pumped up by the pump system. The coater consists of three parts (figure 20). The resin is pumped into the top component. Then the resin is pressed slowly through small holes in the plate and is lead into the bottom part where the thread coating happens. The entire coater is made with parts reused from the TreeD-project.

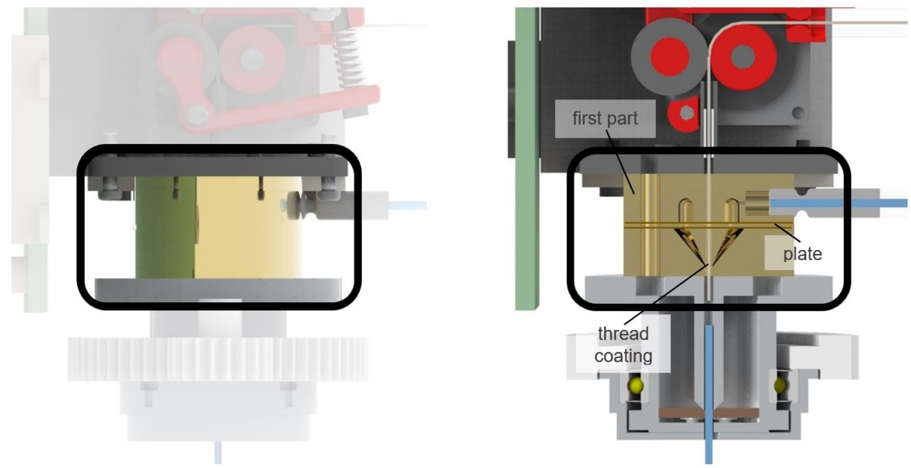

Figure 20: Picture of the coater

Curing
After the coating process, the coated thread is led through a small tube out of the printer head. A circuit board with four UV-LEDs is placed close to the tip of the printer head (figure 21). The curing takes place directly after the thread has exited the printer head. The LEDs shine onto the thread through holes in the bottom plate (figure 22). The coater contains a tunnel for the wires to the PCB.

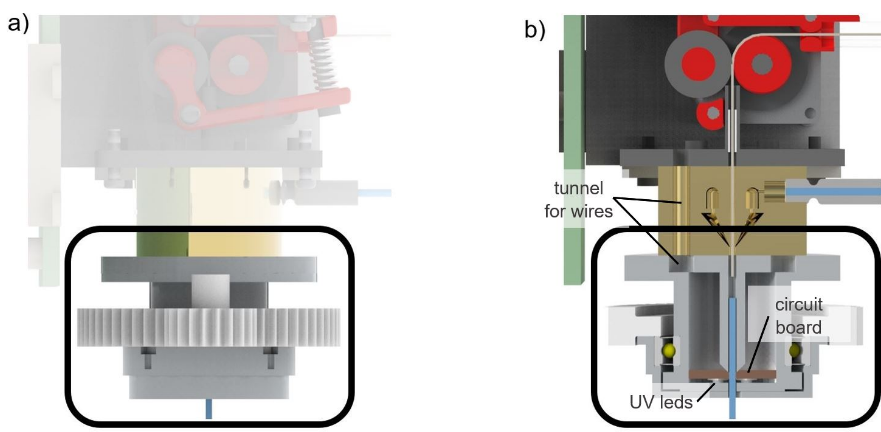

Figure 21: Curing: a) Close-up of the curing mechanism. b) Section-view that shows the circuit board and UV led.

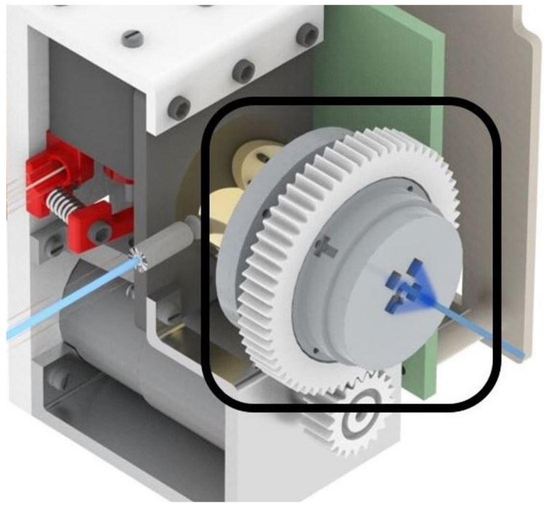

Figure 22: Illustration on how the UV lights hit the thread.

Cutter

The chosen cutter mechanism is based on the concept that is mentioned in section 4.8 Cutter, where two circular plates rotate, while pressed against each other. Instead of rotating plates, there are two cylinders of which one is connected to the coater system and does not rotate. The other cylinder, which is larger, rotates and is connected to a gear. This gear is driven by a smaller gear which is fixed onto the shaft of the DC-motor (figure 23). For a smooth rotation a bearing is placed between the two cylinders.

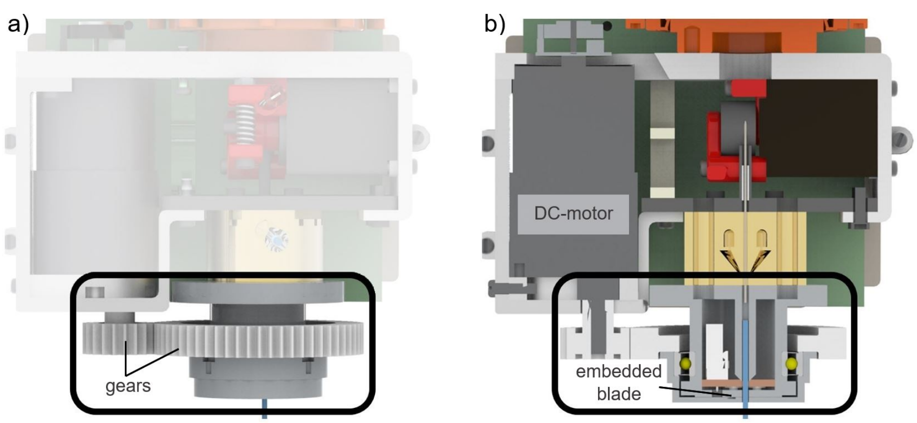

Figure 23: Cutter mechanism: a) Overview of the mechanism. b) Section view of the system

The blade of a scalpel was embedded in the bottom side of the outer cylinder. The blade is fitted into the countersunk pocket that is shown in figure 24. The thread is cut when the driven wheel makes one revolution.

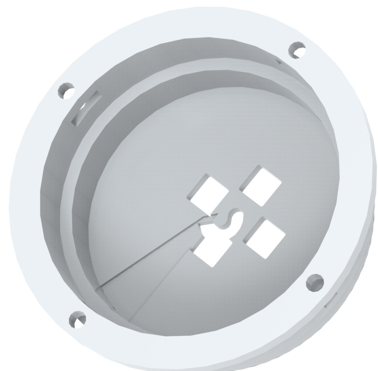

Figure 24: Rotating outer cylinder with the countersunk pocket for the embedded blade

5.4 Pump System

After consideration and testing the chosen concept for the pump was a pressurized system using two pressure sensors, one for the tank pressure and one for the pressure after the valve. The pump system consists of seven parts; a pump, a pressure tank, a solenoid valve, sensors, safety features, a mount and a PCB. The PCB is described in section 5.6 Electronics. The construction is presented in figure 25, however, without tubing, sensors, pump, PCB and safety-valve.

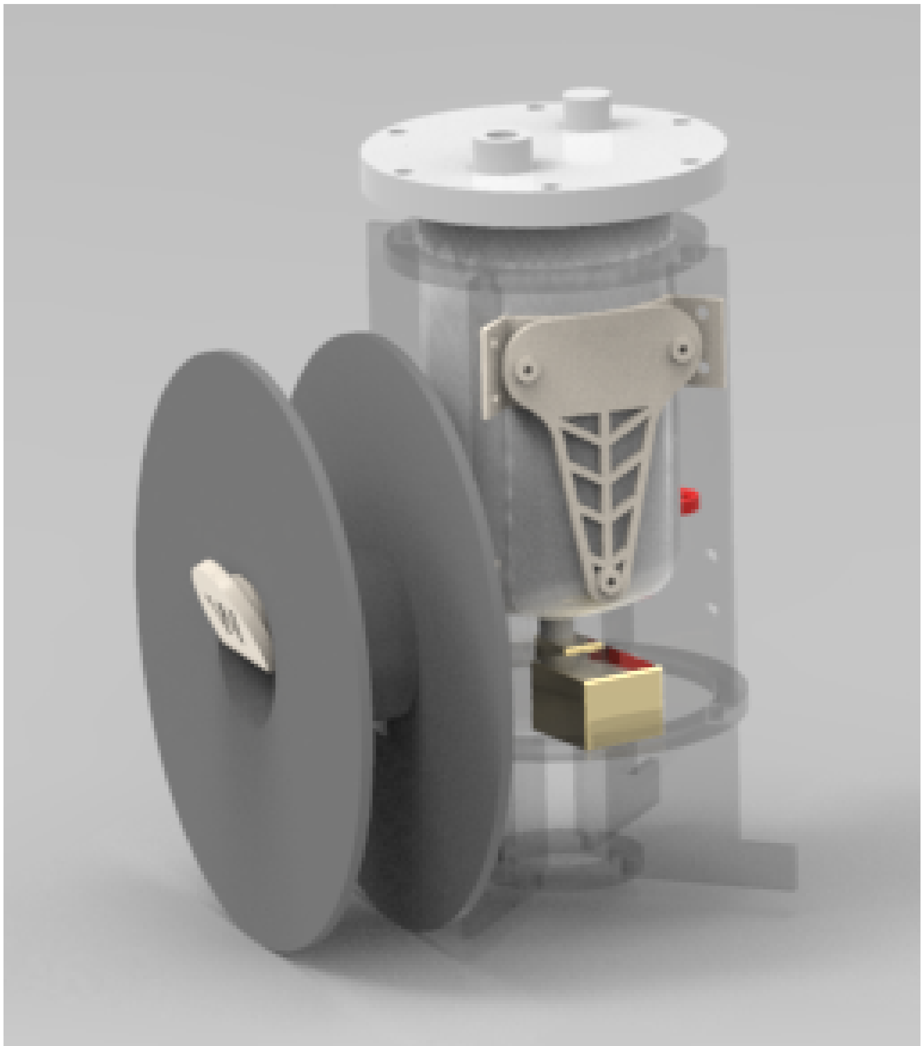

Figure 25: The Pump System

Pump
The pump builds up pressure inside the tank. The motor chosen was a Airpo D2028B which has the ability to provide a maximum of 2.2 bar at 12 L/min to 15 L/min. The pump runs on 12 VDC and rated for continuous operation at 12 W.

Pressure tank
The pressure tank was manufactured in-house to the specifications of being air tight, not to let any UV-light in and having an outlet that resin would natu-

rally enter. The tank was built from stainless steel, pre-manufactured thread adapters, six m6 screws and an O-ring. By tightening the lid and tank together with the previously mentioned screws and the O-ring inbetween, an air tight seal was created, as well as an access point to refill the resin. An exploded view of the tank can be seen in figure 26.

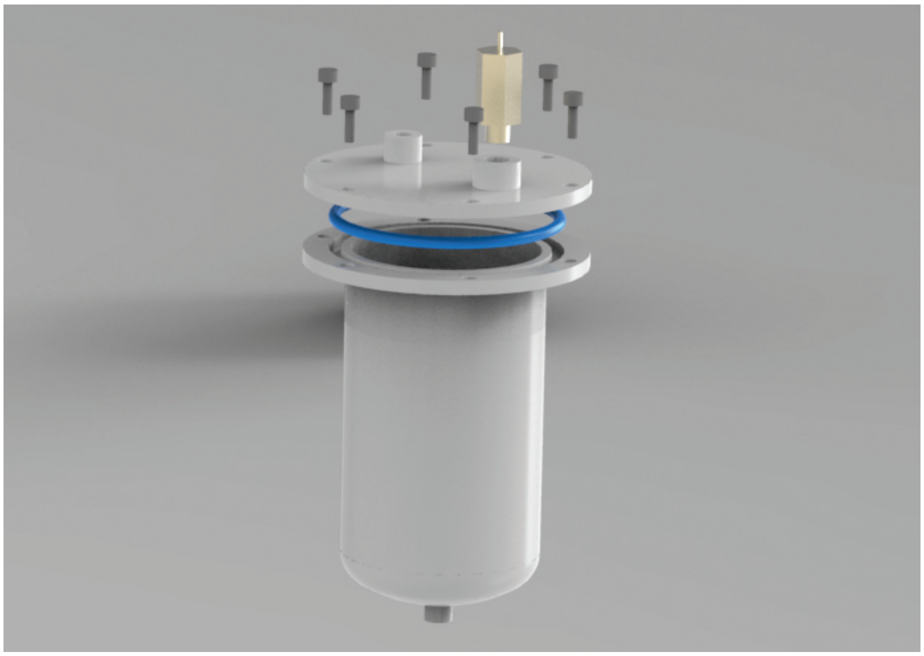

Figure 26: The Pressure Tank

Valve
A valve was connected directly to the outlet of the tank, allowing the resin to be fed without delay and granting the ability of controlling flow. The SMC VX21 used for this is rated for 1 MPa of pressure, designed for oil as medium and operates at 24 VDC and 4.5 W. The rated pressure at nearly five times the maximum pressure was a consequence of the stickiness of the resin, which would otherwise cause the valve to easily get stuck in the open state.

Sensors
Sensors were a vital part for the controllability of the resin feeding system. For this two MXP5700ASX pressure sensors were used which are rated for an absolute pressure of 15 kPa to 700 kPa and placed in parallel with the air inlet and the resin outlet. The sensors ran on 5 VDC and gave an analog output signal from 0 V to 5 V, making them well suited for direct use with the MCU of choice. A 10 bit analog-digital-conversion gave a resolution of 0.6 kPa.

Safety features

Efforts were made to maintain the safety of each part. Wear-resistant colored tubing with an inner diameter of 4 mm was used to connect individual parts together as well as connect the system to the printer head. Wear-resistance limits corrosion and wear from longterm use of the resin, while the non-transparency averts UV-light. The tubing was connected to the individual parts using either tube fittings or nipples. The tubing and fittings where rated at 5 bar to increase redundancies and safety. A mechanically tunable safety valve was fitted on the tank for safety reasons. This was rated for 1 bar to 7 bar and was able to be opened manually. The stress on the pressurized tank is:

$$\sigma = \frac{p_{tank} r}{t}, \tag{4}$$

where p_{tank} is the pressure in the tank, r the inner diameter of the tank and t the thickness of the wall. Under the assumption that the safety valve is set to max (7 bar), the radius being 80 mm and wall thickness being 2 mm the stress was calculated to be 14 MPa. Considering the tensile strength of stainless steel being at least 515 MPa this yields a safety factor of 36.78.

The mount

The tank mount became more than just means of keeping the tank upright. The tank mount was designed to hold the PCB, sensors and the roll of thread that was fed to the printer head as well (figure 27). The mount was made of acrylic sheets and allowed easy access to the tank-top for comfortable mounting and dismounting.

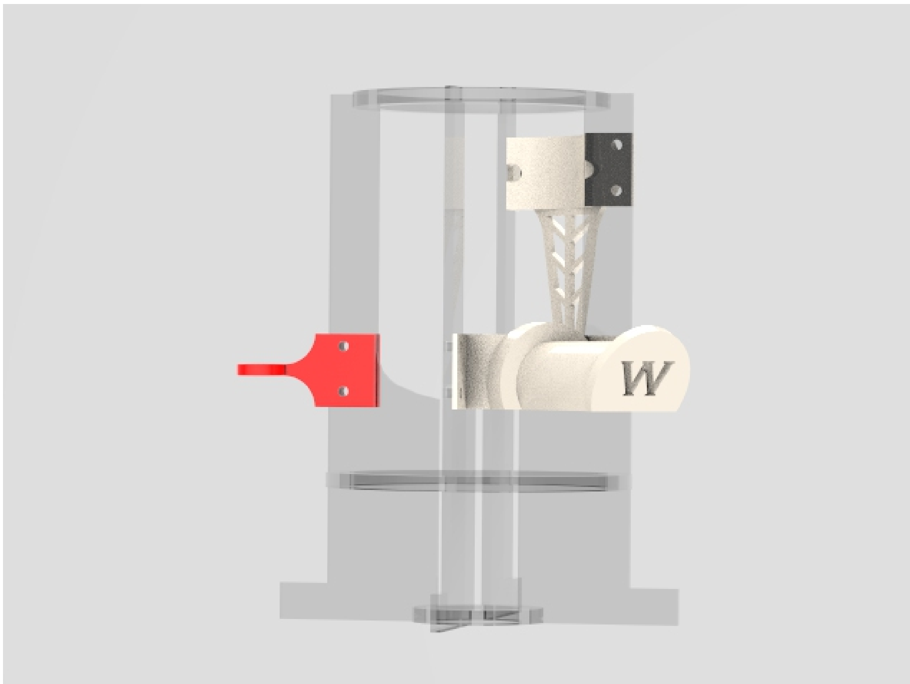

Figure 27: Mount for the Pump System

5.5 Controller

Cutter Control
To find the right parameters, the cutter system was mathematically modeled and simulated using Matlab and Simulink. The modeling was done in two stages: *Motor Dynamics*, describing the dynamics of DC-motor used to drive the gearbox; *Gearbox Dynamics*, describing the dynamics of the gearbox.

Motor Dynamics
To properly control the combined gearbox and DC-motor used for cutting, a suitable sample time T_s needed to be determined. The method used to do this was to model the system mathematically using linear time invariant (LTI) equations, finding the fastest pole of the system and choosing the sample time according to the following equation:

$$T_s = \frac{1}{30\omega_p} \tag{5}$$

Where ω_p is the systems fastest non-zero pole, since a pole in the origin would mean an infinite sample time, which would be impossible to implement.

The modeled subsystems are depicted as follows:

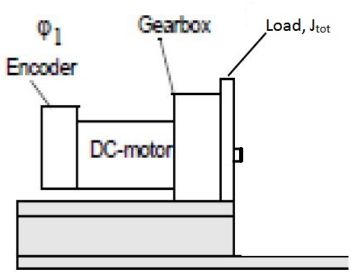

Figure 28: System to be modeled

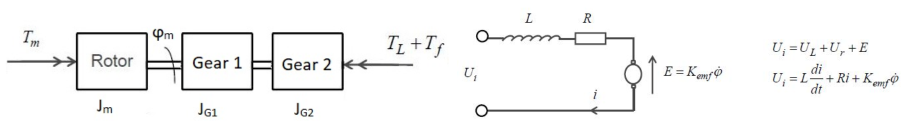

(a) Mechanical model of the cutter motor (b) Electric model of the cutter motor

Figure 29: Consecutive Equations for the DC Motor

The transfer function with voltage U_i as input and motor shaft position φ_m as output is:

$$G(s) = \frac{\varphi_m(s)}{U_i(s)} = \frac{k_t}{sR_a(J_m s + \frac{k_e k_t}{R_a} + d_m)}, \tag{6}$$

Where the parameters are as declared in table 2. The reader should note that the system is quasi-stable, since all poles are located in the left half of the complex plane or in the origin. A model of the system can be seen in figure 30.

Variable	**Description**	**Value**	**Unit**
J_m	Motor inertia	50×10^{-6}	$\mathrm{kg\,m^2}$
R_a	Armature Resistance of the DC motor	8	Ω
k_e	DC-motor electromotive force constant	1.1×10^{-3}	V/rpm
k_t	DC-motor motor torque constant	7.1×10^{-3}	N m/A
d_m	Linear Vicious Friction	35.3×10^{-6}	N m s/rad

Table 2: Model parameters obtained from datasheets or via measurements.

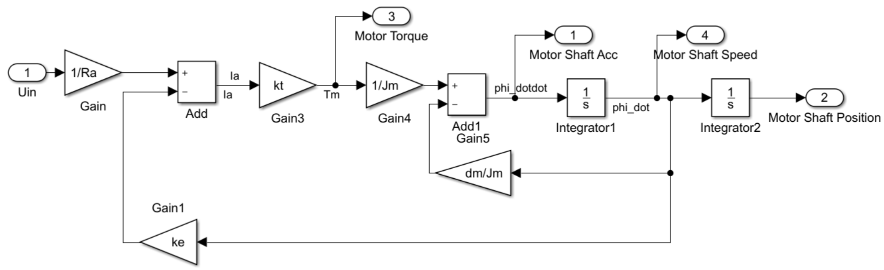

Figure 30: Simulink model of the DC-motor dynamics

A step response of the modeled system was simulated and the fastest non-zero pole ω_p was $-0.0907\,\mathrm{Hz}$.

By using equation 5, the sample time, T_s of the system was decided resulting in $T_s = 3\,\mathrm{ms}$.

Gearbox Dynamics
The gearbox system was comprised of two separate gear stages: a steel gear box and a plastic gear connecting the cutter mechanism and the steel gear, both of which are described in 5.3 Printer head. The gearbox dynamics are modeled via a free body diagram (figure 31).

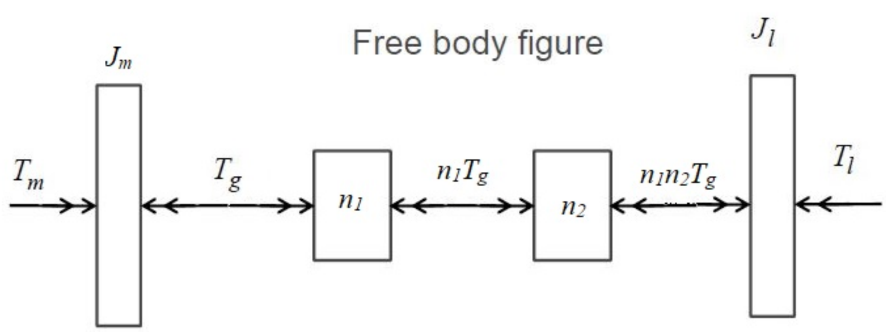

Figure 31: Free body diagram of the torques applied to the motor and gearing.

From the free body diagram, the gear boxes were concluded to reduces the velocity and increases the torque of the output shaft according to equation 7.

$$\begin{gathered} J_m \ddot{\varphi}_m + = T_m - \frac{T_l}{n_1 n_2} \\ \dot{\varphi}_{load} = \frac{\dot{\varphi}_m}{n_1 n_2} \end{gathered} \tag{7}$$

There is a phase shift between the gears position and velocity inside the gear boxes, because of the material skewing, affecting how much power is transfered. The power transfered is given by:

$$T_l = J_l \frac{\ddot{\varphi}_m}{n_1 n_2} + k_{plastic}(\varphi_l - \frac{\varphi_m}{n_2}), \tag{8}$$

Where $k_{plastic}$ is given by equation 9 [22].

$$\begin{aligned} k_{plastic} &= \frac{I_{plastic} G_{plastic}}{l_{plastic}}, \\ I_{plastic} &= \frac{\pi d^4_{plastic}}{32}, \end{aligned} \tag{9}$$

Where $G_{plastic}$ is the shear modulus of plastic used in the gear, $I_{plastic}$ is the polar moment of inertia for the plastic gear and $l_{plastic}$ is the length of the plastic gear.

A model of the gear boxes can be seen in figure 39 and the parameters used for the simulation can be found in table 3.

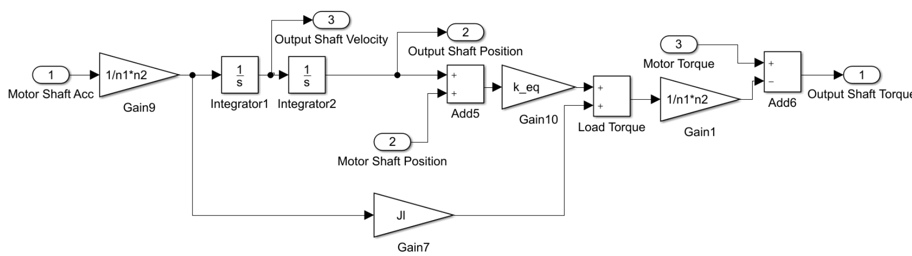

Figure 32: Simulink model of the Gear Boxes dynamics

Variable	Description	Value	Unit
J_l	Inertia of the combined Gear Boxes	4.68	$\mathrm{kg\,m^2}$
$l_{plastic}$	Length of plastic gear	9×10^{-3}	m
$G_{plastic}$	Plastic Shear Modulus	0.117×10^{9}	Pa
$d_{plastic}$	Plastic Gear Radius	18×10^{-3}	m
n_1	Gear box ratio of Steel gearbox	102	–
n_2	Gear box ratio of Plastic gearbox	3	–

Table 3: Parameters from datasheet or provided via measurement used to simulate the gear Boxes.

Simulation Results

The open loop system can be seen in figure 33.

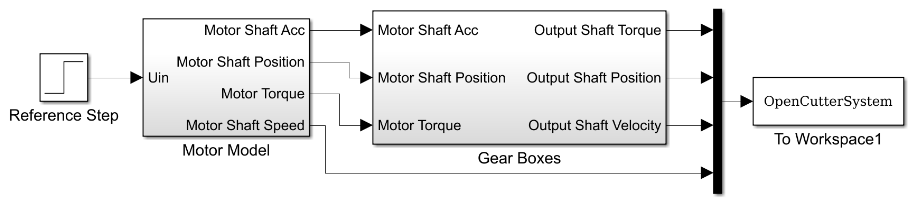

Figure 33: Simulink Model of the Open Loop Cutter System

The system was closed using a PID controller, which can be seen in figure 34.

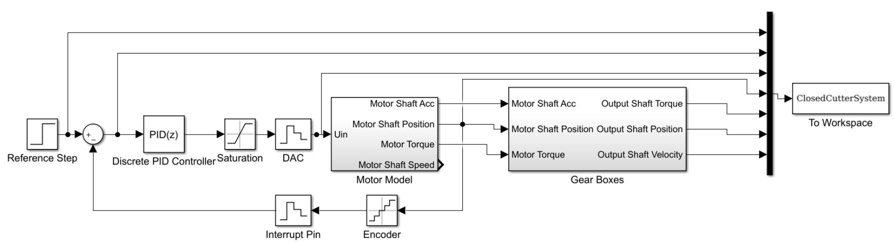

Figure 34: Simulink Model of the Closed Loop Cutter System

A step response was simulated and the rise time and static error were examined. From 4.1 Requirements, the static error has to be low and the rise time has to be fast. The PID gains were tuned until an acceptable result was produced. The control parameters that gave an acceptable result are simulated and the result can be seen in figure 35.

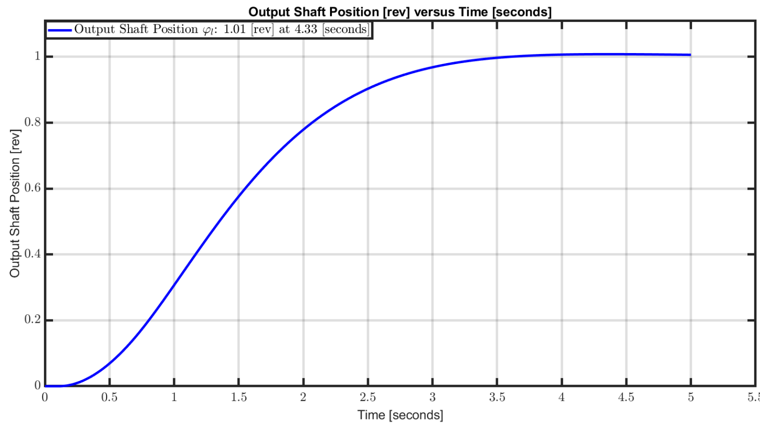

Figure 35: Step response of the closed loop cutter system with a reference value of one revolution

The control signal, error and torque were also plotted to evaluate the plausibility of the signals which can be found in figure 36, 37 and 38.

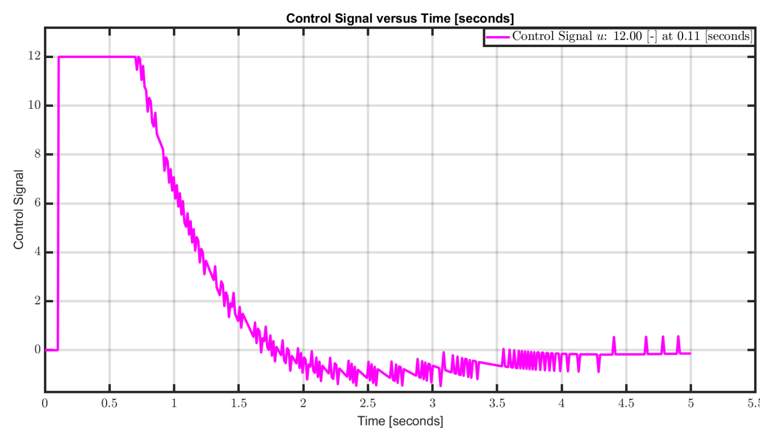

Figure 36: Plot of the control signal to the closed loop cutter system.

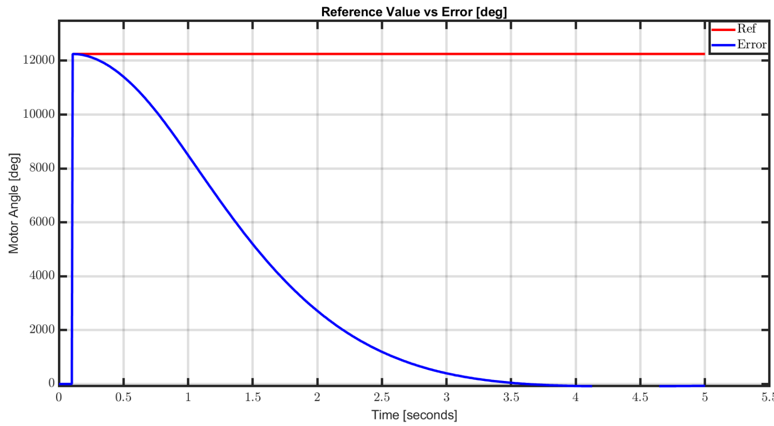

Figure 37: Reference value and error of the closed loop cutter system.

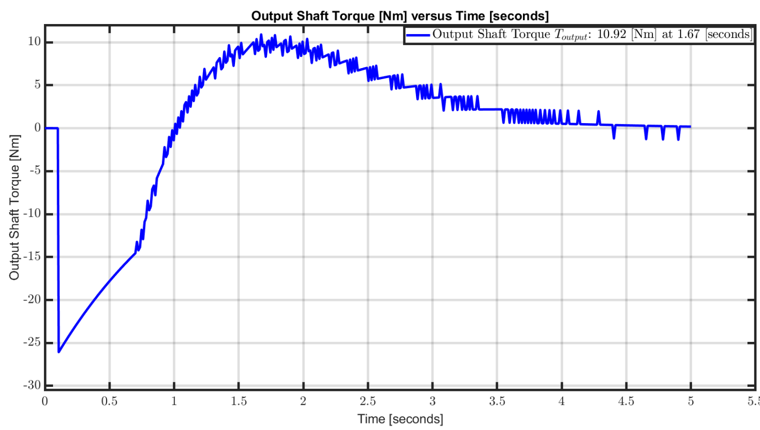

Figure 38: Plot of the torque for the closed loop cutter system.

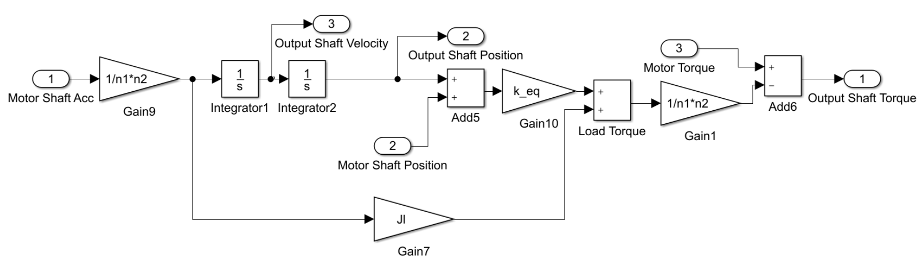

Figure 39: Simulink model of the Gear Boxes dynamics

Control Implementation
The digital PID-controller was implemented using hardware interrupts in order to get precise timing, as mentioned in 4.10 Controller. The controller uses the following difference equation:

$$u[k] = u[k-1] + \alpha e[k] + \beta e[k-1] + \gamma e[k-2] \tag{10}$$

Where $u[k]$ is the kth sampled control signal and $e[k]$ is the kth calculated error. The control parameters α, β and γ are defined as: [23]

$$\begin{aligned} \alpha &= (K_P + K_I \tfrac{T_s}{2} + \tfrac{K_D}{T_s}), \\ \beta &= (-K_P + K_I \tfrac{T_s}{2} - \tfrac{2K_D}{T_s}), \\ \gamma &= \tfrac{K_D}{T_s}, \end{aligned} \tag{11}$$

Where K_P is the proportional gain, K_I is the integral gain, K_D is the derivative gain and T_s is the sampling time, the values of which can be found in table 4.

Variable	**Description**	**Value**	**Unit**
T_s	Control Sample Time	$3.0 \cdot 10^{-3}$	s
K_P	Proportional gain	$2 \cdot 10^{-3}$	-
K_I	Integral gain	$20 \cdot 10^{-6}$	-
K_D	Derivative gain	$1.4 \cdot 10^{-3}$	-

Table 4: Control parameters used for simulation for the cutter.

Pump System Control
To find the right control strategy, the pump system was mathematically modeled and simulated using Matlab and Simulink. The modeling was done in 4 stages: *Tank Dynamics*, describing the dynamics of tank interacting with the pump; *Valve Dynamics*, describing the dynamics of the control valve; *Fluid Dynamics*, describing the behavior of the resin flowing from the tank, via the tube, up to the printer head; *Pump dynamics*, describing the dynamics of the pump. Some simplification were made:

- The pump pressure is always evenly distributed over the surface of the resin inside the tank.
- The resin is incompressible and force propagation is thus instantaneous.
- The tank is filled with 50 % resin and 50 % air at the start of the simulation.
- The temperature of the resin and air is constant at 25 °C throughout the process.

To find the correct sampling time T_s for the pump, the following equation:

$$Ts = \frac{1}{30\omega_p} \tag{12}$$

where ω_p is the fastest non-zero pole in the system.

Tank Dynamics
To get the resin to move, air is pumped into the top of the tank to create an overpressure. As the pressure pushes onto the surface of the resin, the resin starts to move. In figure 40 a simplified model of the energies inside the tank is depicted.

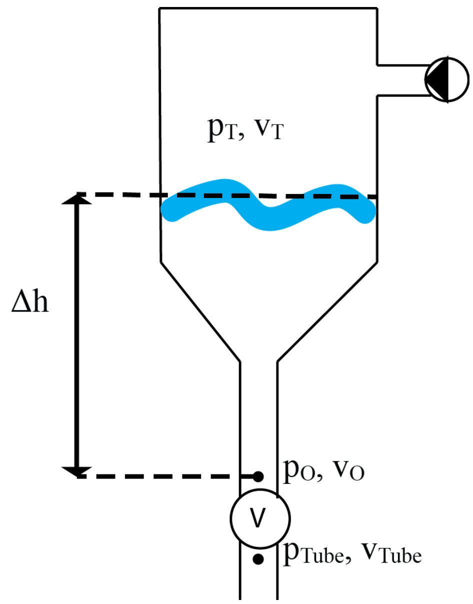

Figure 40: Simplification of the tank system

From figure 40, Bernoulli's equation [24] can be formulated for the tank as:

$$\begin{aligned} \tfrac{v_T^2}{2} + gh_T + \tfrac{p_T}{\rho_{resin}} &= \tfrac{v_O^2}{2} + gh_O + \tfrac{p_O}{\rho_{resin}}, \\ \tfrac{D_T^2 \pi}{4} v_T &= \tfrac{D_O^2 \pi}{4} v_O, \end{aligned} \tag{13}$$

Where v_T is the resins velocity at the resin surface, h_T is the height of the resin surface, v_O is the resins velocity at the tank outlet, h_O is the reference height from the outlet, p_T is the tank pressure, p_O is the pressure at the tank outlet, ρ_{resin} is the density of the resin and g is the gravitational acceleration constant.

By simplifying equation 13 and solving for the pressure p_O results in:

$$p_O = p_T + \rho_{resin} \Delta h g - \frac{v_O^2}{2\rho_{resin}}. \tag{14}$$

A model of the tank dynamics was made and can be seen in figure 41.

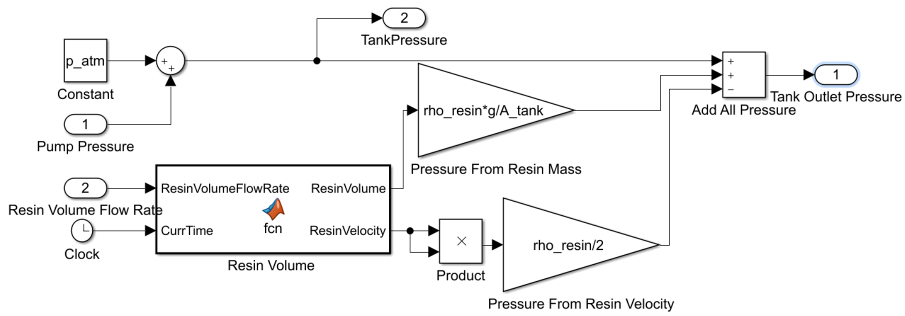

Figure 41: Simulink Model of the Tank Dynamics

All parameters introduced in this section which are needed to run the simulation are presented in table 5.

Variable	Description	Value	Unit	From
A_{tank}	Cross-sectional area of the tank	5.02×10^{-3}	m^2	Measured
A_{outlet}	Cross-sectional area at the tank outlet	4×10^{-3}	m^2	Measured
V_{tank}	Volume of the tank	7.2×10^{-4}	m^3	Measured
ρ_{resin}	Density of the resin	1.12 @ 25 °C	g/cm^3	Datasheet [25]
g	Acceleration due to gravity	9.82	m/s^2	
p_{atm}	Atmospheric Pressure	101 325	Pa	

Table 5: Parameters for tank dynamics from datasheet, calculations or provided via measurement.

Valve Dynamics

The valve used to start and stop the flow of resin can be modeled as a RL-circuit in series (figure 42).

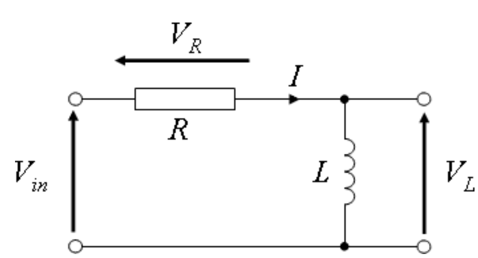

Figure 42: Simplified model of the tank valve.

The transfer function from input voltage V_{in} to output voltage,V_L is given as:

$$G(s)_V = \frac{L_V s}{L_V s + R_V}, \tag{15}$$

Where L_V is the inductance of the circuit, R_V is its resistance and s is a complex number from the LaPlace transform. As the valve is opened, there is a pressure discharge from the tank to the orifice of the valve, resulting in a volume flow, Q_{OT} over the valve, where (O) is a point at the tank outlet before the orifice and (T) is a point after the orifice in the tube, as can be seen in figure 43.

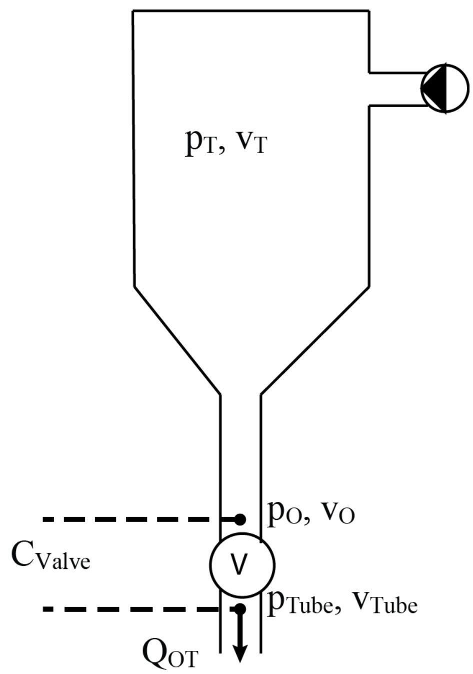

Figure 43: Pressure before and after the tank valve.

The turbulent flow Q_{OT} can be model as:

$$Q_{OT} = C_{valve}\frac{\pi}{4}D_{tube}^2\sqrt{\frac{2(p_T - p_{tube})}{\rho_{resin}(1-d^4)}}, \tag{16}$$

Where C_{valve} is the orifice discharge coefficient, D_{tube} is the diameter of the tube, p_{tube} is the pressure in the tube and d is the ratio between the tank outlet and tube diameter $d = \frac{D_O}{D_{tube}}$. Models of equation 15 and equation 16 can be seen in figures 44 and 45 and all parameter introduced in this section can be found in table 6.

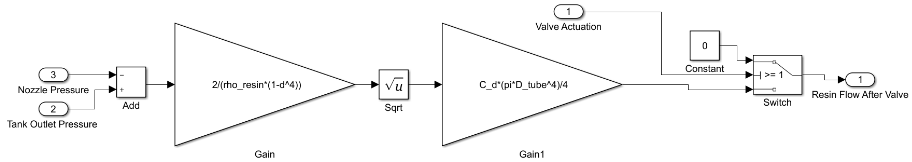

Figure 44: Model of valve dynamics regarding volume flow and pressure

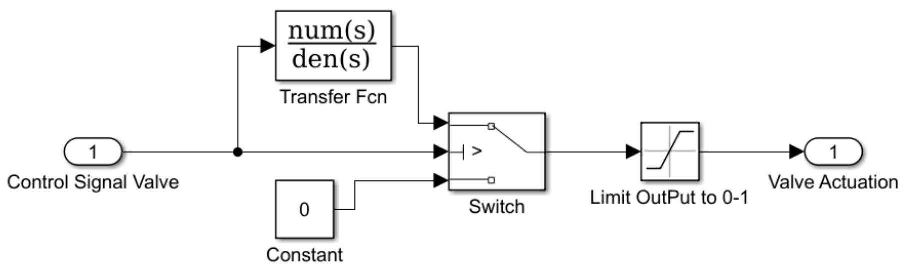

Figure 45: Model of valve dynamics regarding electronics to open and close valve outlet, equation 15.

Variable	Description	Value	Unit	From
R_V	Valve Resistance	122	Ω	Measured
L_V	Valve Inductance	1.225	H	Measured
C_{valve}	Discharge Coefficient of valve	0.23	–	Datasheet [1]
D_{tube}	Tube Diameter	4×10^{-3}	m	Measured
D_{outlet}	Tank Outlet Diameter	8×10^{-3}	m	Measured
p_{tube}	Pressure in the tube	p_{nozzle}	m	Measured

Table 6: Parameters for valve dynamic from datasheet, calculations or provided via measurement.

Fluid Dynamics
The pump system can be modeled as depicted in figure 46.

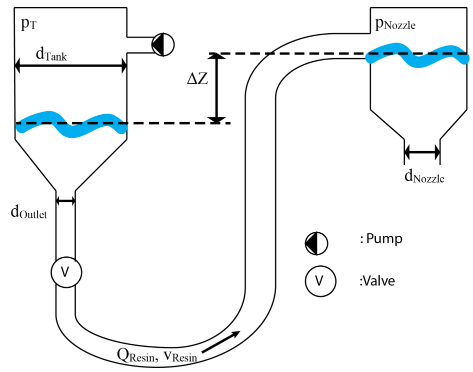

Figure 46: Simplified fluid model.

By manipulating Bernoulli's equation the following description of the system can be derived:

$$H_{Total} = H_s + H_d + (p_T - p_{nozzle}), \tag{17}$$

Where H_{Total} is the total pressure head, H_s is the total static pressure head, H_d is the total dynamic pressure head, p_T and p_{nozzle} are the pressure at the tank and the nozzle, respectively.

The static pressure head is the level difference between the reference level and the upper boundary, as seen in figure 46 and may be calculated as

$$H_s = \frac{\Delta z}{\rho_{resin} g}, \tag{18}$$

Where Δz is the distance difference from a reference level.

The dynamic pressure head can be calculated as:

$$H_d = \frac{K v_{resin}^2}{2g}, \tag{19}$$

Where K is the total friction coefficient and v_{resin} is the average velocity along a streamline inside the tube. The average velocity in the tube is defined as:

$$v_{resin} = \frac{Q_{OT}}{A_{tube}}, \tag{20}$$

Where Q_{OT} is the flow rate over the valve and A_{tube} is the tube's cross-sectional area.

To determine the total friction coefficient K, the following definition was used:

$$K = K_{static} + K_{dynamic}, \tag{21}$$

Where K_{static} is the friction coefficient due to static friction factors (e.g fittings and valves) and $K_{dynamic}$ is the friction due to the tube. K_{static} can be determined from static coefficient tables, and is determined as:

$$\begin{aligned} K_{static} &= K_{valve} + 2K_{entrance} + K_{coater}, \\ K_{coater} &= K_{90^o bend} + 5K_{entrance} + 4K_{45^o bend} + K_{outlet}, \end{aligned} \tag{22}$$

Where the static coefficients can be found in figure 47a and 47b. The values of the coefficients can be found in table 7.

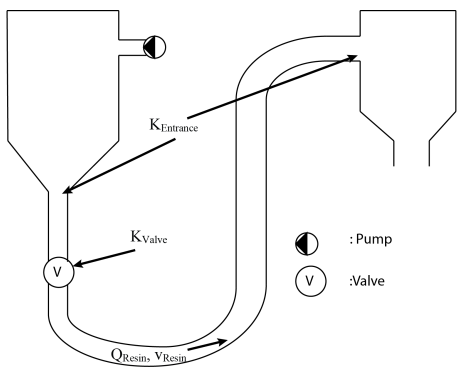

(a) Static Friction coefficients in the pump system

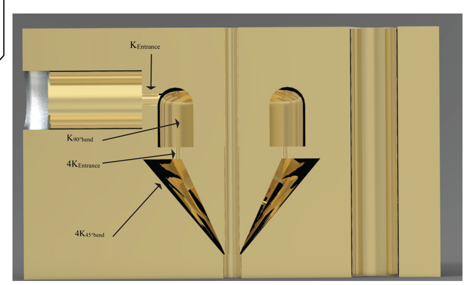

(b) Static Friction coefficients in the coater

Figure 47: Static Friction Coefficients and where to find them in the pump system

Variable	Description	Value
K_{valve}	Butterfly Valve	0.3
$K_{entrance}$	Pipe Entrance (bellmouth)	0.05
K_{outlet}	Bellmouth Outlet	0.3
$K_{90^\circ bend}$	90° Bend (short radius)	0.75
$K_{45^\circ bend}$	45° Bend (short radius)	0.3

Table 7: Static Friction Coefficients from datasheet [1]

To find the dynamic friction in the tube, the following equation can be used:

$$K_{dynamic} = \frac{fL_{tube}}{D_{tube}} \tag{23}$$

Where L_{tube} is the tube length, D_{tube} is the tube diameter and f is the friction coefficient between the fluid and the tube. The friction coefficient is dependent on if the flow is laminar or turbulent, which can be determined via the Reynolds number. If $Re < 2000$, then the flow is defined as “laminar” flow, $Re > 10000$ the flow is defined as “fully developed turbulent” flow, and any Reynolds number values between 2000 and 10000 as “transitional” flow [24]. The Reynolds number is defined as:

$$Re = \frac{v_{resin} D_{tube} \rho_{resin}}{\nu} \tag{24}$$

Where ν is the kinematic viscosity of the resin. From section 4.7 Resin feeding, the flow rate Q_{resin} of the resin is between 49.1 µL/s to 98.2 µL/s. Using equation 20 and 24 results in a Reynolds Number between 0.03 and 0.06, meaning the flow is defined as strictly laminar. The reader should note that this is only true ”far” after the valve opening, where the fluid is most certainly turbulent [1].

For a laminar flow, the friction coefficient f is defined as:

$$f = \frac{0.25}{log[(\frac{R_{tube}}{3.7D_{tube}}) + (\frac{5.74}{Re^{0.9}})]^2}, \tag{25}$$

Where R_{tube} is the roughness factor of the tube. A model to describe the fluid dynamics can be seen in figure 48 and every parameter introduced in this section is summarized in table 8.

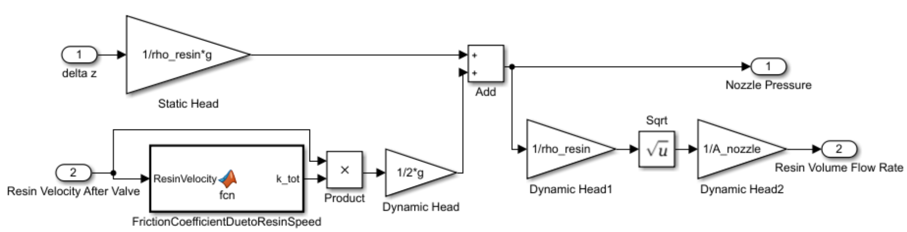

Figure 48: Model of the fluid dynamics regarding the tube and printerhead

Variable	Description	Value	Unit	From
K_{static}	Static friction coefficient	3.3	–	Equation 22
ν	Resin Kinematic Viscosity	0.9	$\mathrm{N\,s/m^2}$	Datasheet [25]
D_{tube}	Diameter of tube	4×10^{-3}	m	Measurement
L_{tube}	Length of tube	3.6	m	Measurement
D_{nozzle}	Cross-sectional area of nozzle outlet	8×10^{-3}	$\mathrm{m^2}$	Measurement
R_{tube}	Roughness factor of plastic tube	7×10^{-6}	m	Datasheet

Table 8: Parameters for fluid dynamic from datasheet, calculations or provided via measurement.

Pump Dynamics

The pump performance was measured using the pressure sensor, described in section 5.4 Pump System. A known voltage between 0 and $V_{max,pump}$ was applied and the accumulated pressure was plotted versus time. The result can be seen in figure 49.

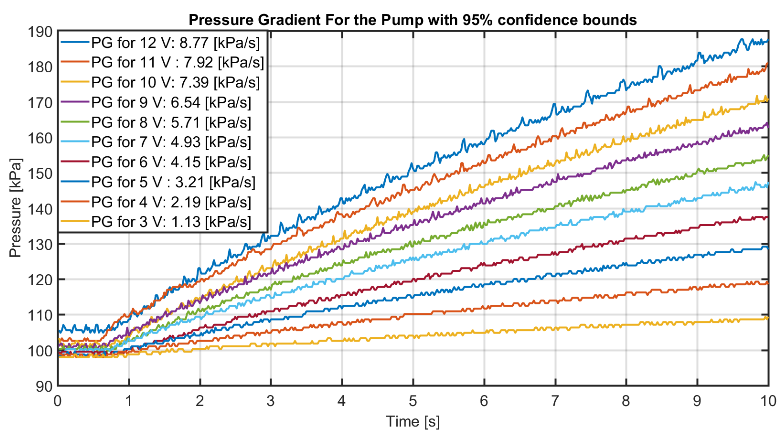

Figure 49: Pump output pressure gradient.

As seen in figure 49, the pressure is linear versus the applied voltage with the factor Ψ_i with 95 % confidence bounds, where $i \in [3, 4, \ldots, 12][V]$. The results were used to identify the plant of the pump as

$$G_{pump,i}(s) = \frac{p_{pump}(s)}{U_i(s)} = \frac{1}{(\Psi_i s + 1)}. \tag{26}$$

Simulation Results

The full model of the open loop system can be seen in figure 50.

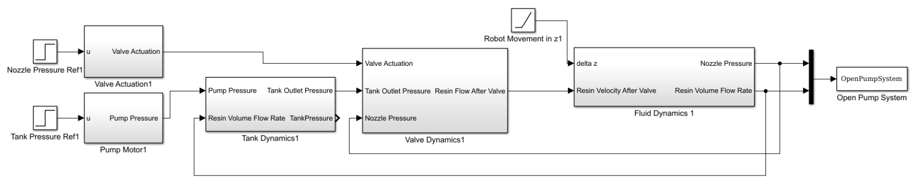

Figure 50: Open loop model of the pump system

The pump pressure, resin volume flow rate, tank pressure and analog signal to the valve for the open loop system were plotted and seen in figure 51, 52 53 and 54.

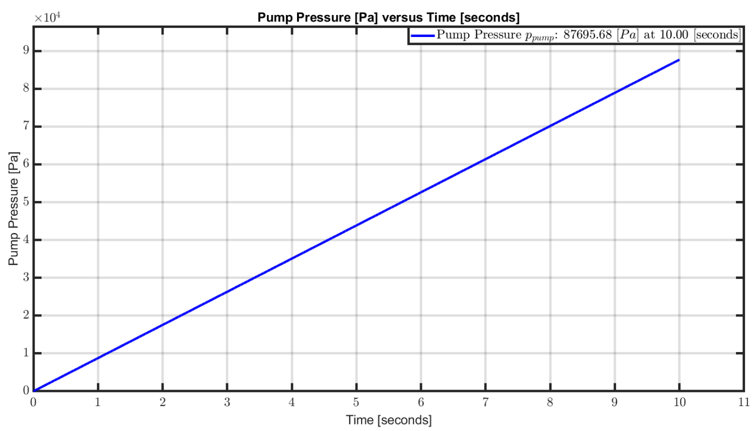

Figure 51: Pump pressure of the open loop pump system

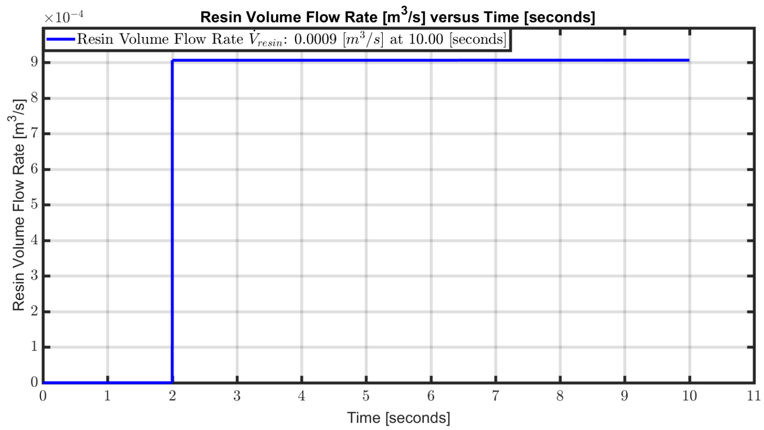

Figure 52: Resin volume flow rate of the open loop system.

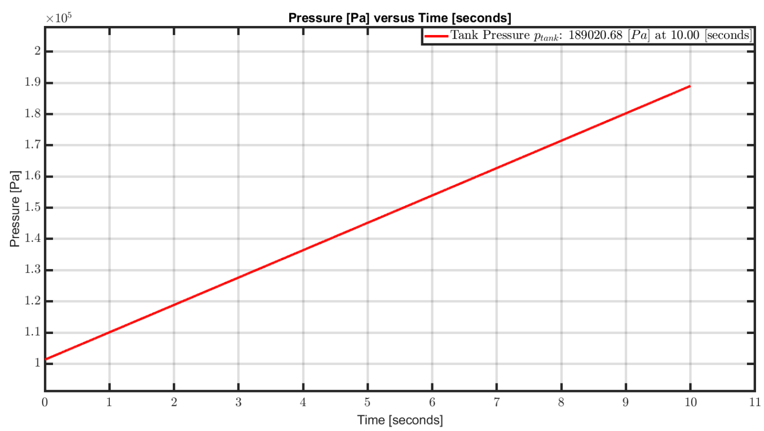

Figure 53: Tank pressure of the open loop pump system

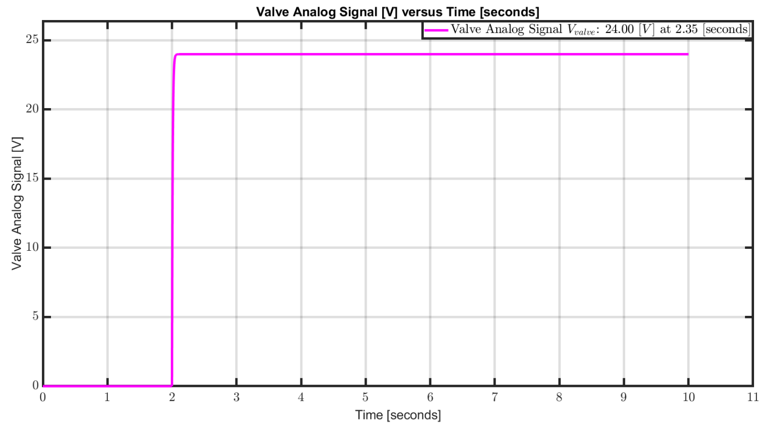

Figure 54: Analog signal to the valve for the open loop pump system

The full modeled pump system was closed via an analog filter that was implemented to reduce the noise from the sensor readings, where the transfer function of a low pass filter from the input V_{in} to the output V_{out} is given as:

$$G_{LP}(s) = \frac{1}{s + \omega_{cutoff}}. \tag{27}$$

The cut-off frequency of the low-pass filter was determined using Nyquist–Shannon sampling theorem [26], as:

$$\omega_{cutoff} = \frac{1}{2T_{s,pump}}. \tag{28}$$

The closed system can be seen in figure 55.

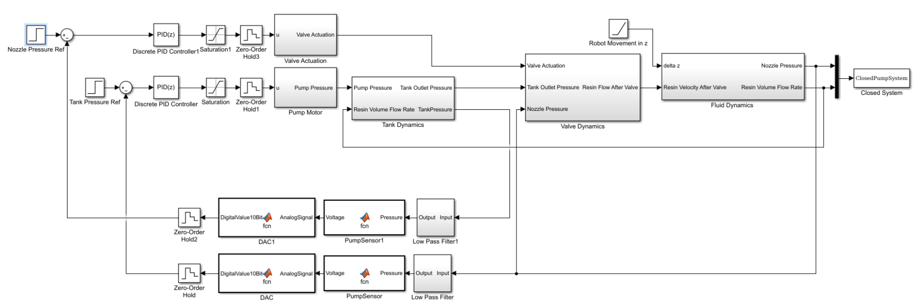

Figure 55: Closed model of the pump system

Controller Implementation
The controller used the same control implementation as mentioned in section 5.5 Controller.

To choose the sample time T_s, the fastest pole are most likely to be in the pump or valve dynamics, since the tank and fluid dynamics are slow physical systems, while the pump and valve are electric ones. Using the equation 26 and 15 gives:

$$
\begin{aligned}
G_{pump,12} &= \frac{1}{s+\frac{1}{\Omega_{12}}} \\
G_{valve} &= \frac{L_v s}{s+\frac{R_v}{L_v}}
\end{aligned}
\tag{29}
$$

By using equation 12 the sampling time was calculated to $T_s = 33.47\,\text{ms}$.

5.6 Electronics

Printer Head PCB

The PCB on the printer head contains the MCU that controls the subsystems on the printer head. Additionally, the PCB contains all the interfaces the MCU needs for driving these subsystems, the interfaces for communicating with the IRB controller, communicating with the pump station and the power converters to supply all these components with the needed voltages. The board schematic of the PCB is shown in figure 56.

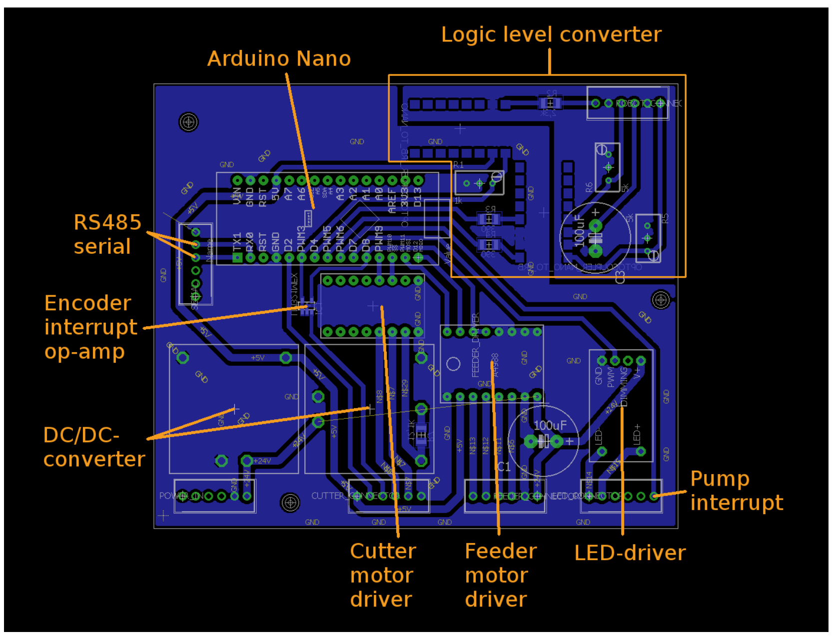

Figure 56: Schematic of the printer head PCB.

The MCU and motor drivers are connected to the board with PCB-sockets. An Arduino Nano was used as MCU.

To drive the motor for the feeding an Pololu A4988 stepper motor driver was used. An 16-Bit timer of the Arduino Nano was used to control the step and direction input of the driver which in turn sends out signals to the motor.

The motor used for cutting the thread is driven by a Pololu DRV8833 dual motor driver, of which only one channel is used. The driver does get its input from a 16-bit timer of the Arduino Nano. The two encoder signals were connected to the Arduino Nano, however one does need to be wired via a unity gain op-amp, because the signal has to share the pin with the interrupt from the IRB. Otherwise not enough current to the pull-down resistor can be provided. In the end, this channel was not used. The outputs from the driver are routed to a connector where the wires from the motor are connected.

For communication with the IRB controller, RS485-serial communication and three interrupts were used. One interrupt from the robot to the printer head and two from the printer head to the robot. To enable the serial communication the RXD and TXD pins of the Arduino Nano were routed to a connector, which was wired to the IRB's serial port via an RS232-RS485 converter. To send interrupts between the IRB and the Arduino Nano the 5 V logic voltage level of the Nano has to be converted to the 24 V logic level of the robot. For this purpose two Vishay ILQ2 optocouplers were used. The optocouplers also provide electric separation between the robot and the printer head electronics, so that they do not have to use the same ground. The schematic of the logic level converter is shown in figure 57. R_1 is chosen such that the current into the optocoupler is 10 mA. R_2 is a pull-down resistor with a value high enough that the current from the optocoupler creates the desired output voltage.

The interrupt from the printer head to the pump station is wired directly between the two Arduino Nanos of the different subsystems.

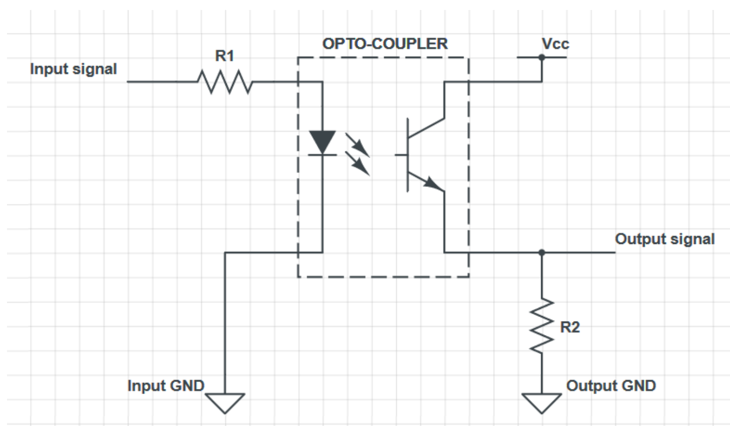

Figure 57: Schematic of the logic level converters.

To drive the LEDs of the hardening mechanism a Recom RCD-24-0.70 LED-driver was used. The intensity of the LEDs is controlled by a PWM-signal controlled by the 8-bit timer of the Arduino Nano.

The board has an input of 24 V. To provide all the components with their required voltages the input voltage is converted to 12 and 5 V, using a Recom RP15-2405SA and a RPA30-2412SAW DC/DC-converter, respectively. The 12 V is trimmed down to 10.8 V.

Pump PCB

The PCB at the pump station contains an MCU that controls the pump and the valve. In order to do this the PCB also contains a driver for the pump motor, a switch for the valve, anti-aliasing filters for the pressure sensors and DC/DC-converters to supply these parts with power at the correct voltages. The board schematic of the PCB is shown in Figure 58.

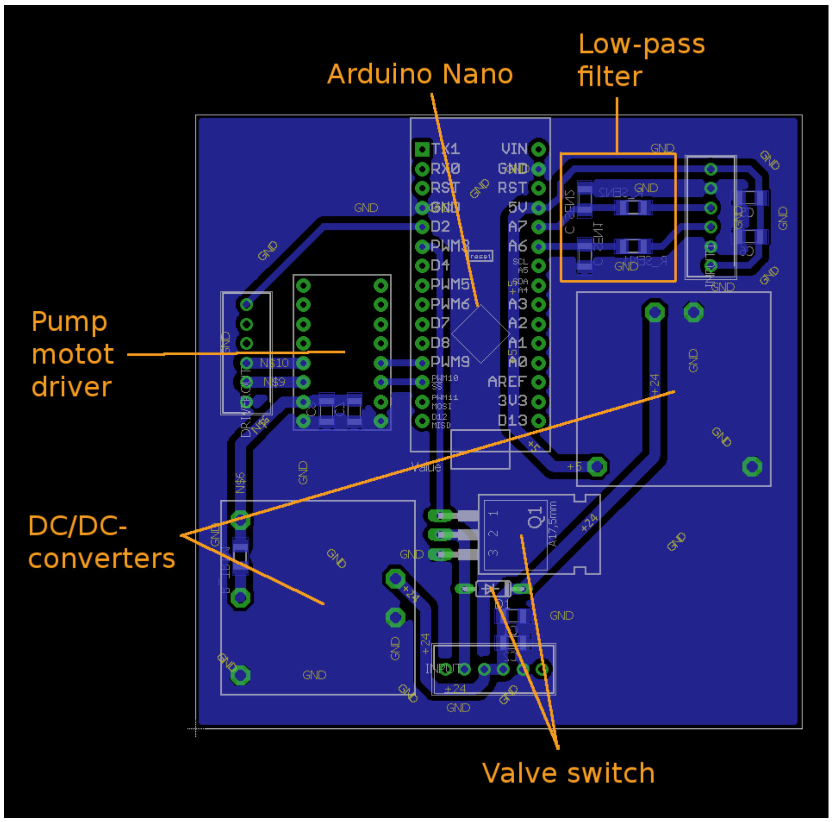

Figure 58: Schematic of the pump PCB.

The MCU and motor drivers are connected to the board with PCB-sockets. An Arduino Nano was used as MCU.

The motor used for creating pressure in the tank is driven by a Pololu DRV8833 dual motor driver, of which only one channel is used. The two input signals to the driver was set by a 16-bit timer of the Arduino Nano. The OUT pins of the driver are routed to a connector where the are connected to the wires from the motor.

For controlling whether the valve is open or closed a simple bipolar transistor and a free wheeling diode were used. The base of the transistor was connected the Arduino Nano and controlled by the 8-bit timer.

The signals from the pressure sensors are filtered by anti-aliasing filters using a cut-off frequency of 64 Hz. The filters are passive RC low-pass filter with a resistance of 530 Ω and a capacitance of 4.7 µF.

The board has an input of 24 V. To provide all the components with their required voltages the input voltage is converted to 12 and 5 V, using a Recom RP15-2405SA and a RPA30-2412SAW DC/DC-converter, respectively. The 12 V is trimmed down to 10.8 V.

5.7 Software

The software in this project was written on three different platforms, RobotStudio, the printer head's MCU and the pump's MCU. In this system, RobotStudio is the master and the MCUs are slaves. The purpose of RobotStudio is to store and send commands to the MCU and control the robot arm. The purpose of the printer head's MCU is to translate the commands received from RobotStudio and relay that information to other subsystem according to the received command. Lastly, the purpose of the pump MCU is to start pumping when an interrupt is received from the printer head's MCU. It also regulates the pressure in the tank and the nozzle to control the resin flow.

Robotstudio Software
ABB robots have a default software that is called RobotStudio [27] which is used in this project. This software is used to generate paths instructing the robot with movements. This is done by creating points in a virtual environment where the robot can be simulated. An overview of the virtual environment is shown in figure 59 below.

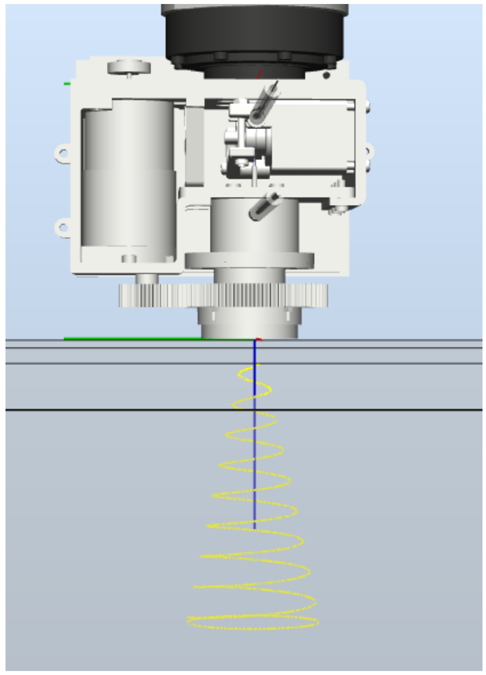

Figure 59: A picture of how the virtual environment looks like. The yellow lines represents the paths in which the robot shall move in.

Points are connected into paths, which in turn generate instructions on how the movement is to be conducted, for example the direction of the movement, translational speed of the robot arm and the configuration the robot shall have throughout the motion. Movements can be simulated in robot studios, providing a visual confirmation that the desired motions are in fact achieved. When the desired paths have been created and simulated, the data generated in the virtual environment can be re-generated into computer code which in turn could be manipulated for use in this project. Said manipulation was an essential part in making communication feasible.

Communication was implemented via I/O and COM ports by manipulating the generated code via a programing language called RAPID. This language is an ABB standard code language for ABB controllers.[28]

There are three major steps the robotstudio's software have to go through in order to realize the desired movement and communication. Please refer to the flowchart over the robotstudio software in Figure 60.

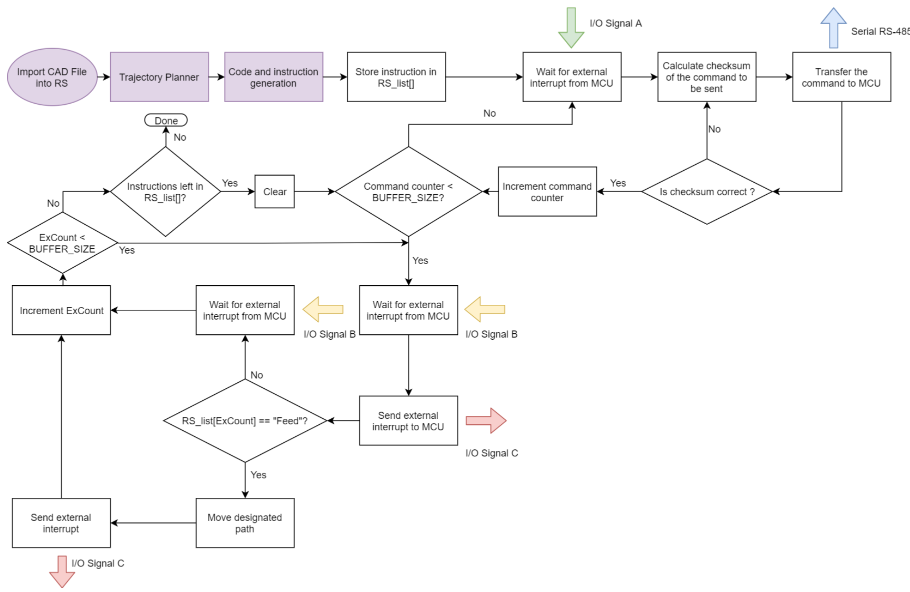

Figure 60: Flowchart of the robotstudio software.

The first step is a preparatory phase where the paths are generated according to the desired shape the 3D-printer shall print in robotstudio's virtual environment. This is were commands like "Feed", "Move" and "Cut" (all of which are developed specifically for this project) are planned out and hardcoded into the generated code.

The second step is to send the hardcoded commands to the MCU via the COM port until the MCU's buffer is full. Between each message sent the robot waits for the MCU to notify via an interrupt that it is ready to receive a new message, allowing the robot to carry on and send a new message.

Before each command is sent a checksum is calculated. The checksums purpose is to make sure that the correct data has been sent. This is achieved by attaching the checksum to the command string before the message is sent. The printer head MCU will then recalculate the checksum and compare if the results are the same. Depending on the result, different types of interrupts are sent to notify the robot if the data sent was corrupt or not. If the checksum is correct the robot continues on with its instruction. However, if the checksum is not correct the robot sends the same message again until the checksum is correct.

The third step is to execute the commands stored by the MCU. How this takes place depends on the command to be executed. If the command is either "Feed" or "Move" the robot moves in accordance with the path it is currently on. When the robot has completed its path an interrupt is sent to the MCU, signaling that the movement has been executed. However, if the command is ”Cut”, the robot shall stand still and await an interrupt from the MCU, signaling that the cut has been made.

Because the MCU has a limited buffer size, all the commands in the command list can not be executed at once; only so many commands can be executed at a time, leading to steps two and three having to be repeated until the command list eventually becomes empty.

Printer head MCU Software

The MCU needs to go through three main steps in order to get a successful print. The flowchart of the printer heads MCU is presented in figure 61.

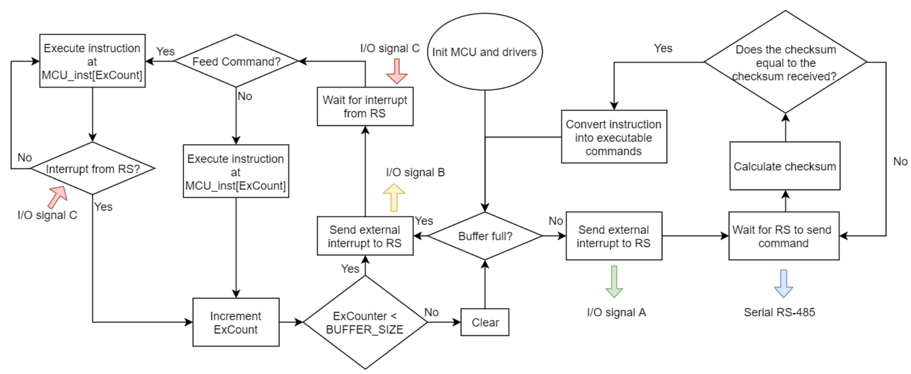

Figure 61: Flowchart of the printer head’s MCU:s software.

The first step for the MCU is to initialize drives, pins and timers that are to be used.

The second step is where the MCU receives commands. First, the MCU sends an interrupt to the robot to notify that it is ready to receive a command. When a command is received it is translated into instructions that the MCU can understand; those commands are then stored in a list. This process repeats until the buffer is full.

The third step is to execute the commands stored in the list. Depending on the command received different actions are taken. If the command is ”Feed” the MCU does two things. First, an interrupt is sent to the pump MCU ordering resin to the nozzle. Then the stepper motor is initialized so that the thread feeding starts. The speed in which the thread shall be fed is stored in the ”Feed” command that the robot sends. The stepper motor stops when the MCU receives an interrupt from the robot (signaling that path has been completed).

If a "Cut" command is received the MCU starts the DC motor and spins it one revolution. This is regulated by a control loop, described in section **?? ??**. When the cutting is complete, the MCU sends an interrupt to the robot to notify that the procedure is done.

When the MCU executes a "Move" command it remains idle until an interrupt is received from the robot.

When the list of commands is empty the second and the third part are repeated.

Pump MCU Software

The pump MCU acts a slave in the system and runs two error-feedback control loops (both of PI-type); one for maintaining a constant pressure in the tank and one for controlling the pressure after the valve, which (given the assumption that there are no leakages) is the same as the pressure in the nozzle resin chamber. Refer to the flowchart in figure 62 below as the software-implementation is explained.

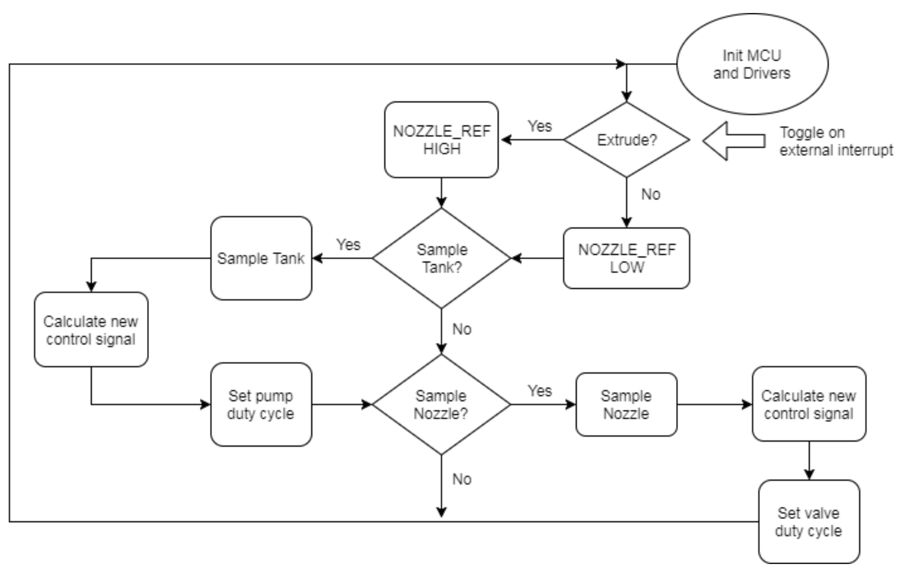

Figure 62: Flowchart over the pump MCU:s software.

The software can be seen as operating in two different states, toggling between the two on the event of an external interrupt which it receives from the printer head MCU. The interrupt simply informs the pump MCU whether it is time to move resin out of the system or not; the pressure reference after the valve (referred to as `NOZZLE_REF`) is then set accordingly. The pressure reference for the tank remains constant.

A significant property of the software lies in setting and clearing two flags at known frequencies through the use of timer interrupts. The state of said flags answer whether or not is time to sample tank and nozzle pressures - in other words sampling frequency is controlled in this manner.

The control loops assure the following behavior of the pump system:

- When `NOZZLE_REF` is high the duty-cycle of the valve will leave it increasingly open. As resin starts flowing the pressure in the tank will drop, causing the pump to work harder. Resin will be forced to the nozzle, ideally at a constant pressure.
- When `NOZZLE_REF` is set low the valve closes, stopping the resin flow and also the need for the pump to run.

6 Verification & Testing

A variety of tests have been done regarding the different parts of the system, but also with the system as a whole. In this chapter, the different tests that have been done are described. For the results of respective test, see Section 7. Results.

6.1 Material

The material's feasibility and properties for printing were tested by a manual construction test and a stress test respectively.

Construction Test
For the construction test of the material two shapes where constructed, a spiral and a cube. They were chosen to specifically mimic what was intended to be printed in section 6.3 System Test.
The manual construction of the cube was done by cutting 12 identical pieces of thread at 55 mm of length, dipping each individual piece in resin and then hardening them with UV-light. Each piece was later assembled by adding resin to the end and pushing the ends of the pieces together and hardening them with the UV-light. This was repeated until a full cube was assembled.
The spiral was built using a continuous thread of approximately 110 cm, by winding it around an aluminum can with a diameter of 5 cm. The thread was treated with resin and later cured with UV-light. The spiral was removed from the can and was treated with another iteration of adding resin and hardening it, since they can spread the resin unevenly over the thread. After being cured a second time the spiral was deemed ready.

Stress Test
In order to perform a stress test, adequate test pieces had to be manufactured. The test pieces were produced by using acrylic mold and manual work. Four test pieces were made; the first with pure resin and the second with the thread oriented perpendicular to the drag direction. The third and the fourth were constructed with the thread oriented parallel to the drag direction but with different ratio of thread to resin, 50% and 40% approximately. The acrylic mold was made with a laser cutter, using the measurements found in figure 63. The thread and resin were later put in the mold with respect to orientation and ratio and then cured in an UV-oven for 159 minutes each. The hardened test piece was then removed from the mold to be tested. The test pieces had a thickness of 3mm and can be seen in figure 64.

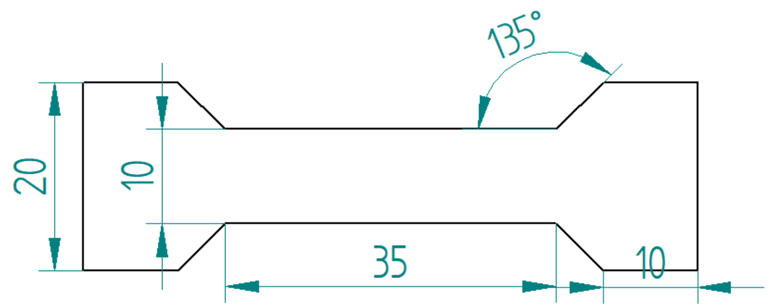

Figure 63: Measurements of the Stress Test Test Piece

Figure 64: Picture of the Actual Test Pieces

The test itself was conducted at Innventia using their equipment. The test piece was mounted in the a test machine. The machine pulled the piece in opposite directions until the test piece broke. Recorded by the machine was the force and translational movement. Using the the known cross-sectional area and previous information the stress was calculated. Only three of the pieces were tested since the one with the grain perpendicular to the drag direction broke in the hand of a team member.

6.2 Thread Feeding

The thread feeding mechanism is a crucial part of the system. Therefore, tests were made to study the functionality of the designed feeding mechanism.

The test methodology used was *Design of Experiments* [29]. The goal of the experiment was to evaluate the precision of which thread was fed via the system and how the fed thread was affected by varying two parameters; feeding speed and spring tension.

Boundary values for speed were chosen in accordance with the required print-speed (LOW) and going as fast as the stepper motor would allow (as specified by the data-sheet) (HIGH). The lower boundary for spring tension was chosen as the minimum tension required for the feeder to grip the thread. The higher boundary was arbitrary chosen to be significantly higher.

The experiment itself was carried out in the following steps:

1. Choose one of the four parameter configurations.
2. Feed thread to the point where it exits the nozzle.
3. Apply a marker to the thread at the outlet, indicating the starting point.
4. Feed a theoretically known length (in this case 5 full revolutions from the stepper motor which corresponds to 123 mm). Make another mark on the thread at the outlet, indicating the actual length of the fed segment.
5. Repeat step four 15 times.
6. Cut off the entire length of fed thread and divide it into the 15 segments indicated by the marks.
7. Measure the segments and repeat the entire process for the remaining three parameter configurations.

6.3 System Test

Once all the parts were assembled, the testing of the complete system could start. The main goal for the tests was to see how the different parts worked together and if the results were similar to the expected outcome.

The test included two different prints. The first print was a spiral and the other was a box, see Figure 65.

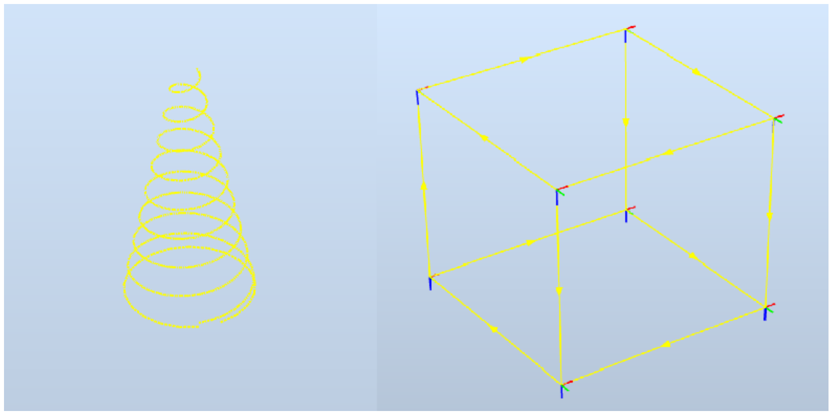

Figure 65: The two objects to be printing during the testing of the system. A spiral print is shown to the left and a box to the right.

The test consisted of that the user started the system and let the system print either the spiral or the box mentioned above. This means that the communication between the various subsystems, as well as the physical aspects of the system had to be fully functional. The aim of the test was that the printer successfully could print a spiral without any need for assistant by the user.

6.4 Verification

Verification tests were done to see if the complete system fulfilled the given requirements.

Methodology
The extensive procedure of testing the system included several test-disciplines and naturally differed with regards to the system level of the subject at hand. However, a bulk of the conducted testing shares a common approach; empirically verifying an expected outcome relating directly to a requirement *or* consequential functionality. This concerns SIL, PIL and HIL testing (including both unit and function tests) but there are specific cases that fall outside of said commonality. Tests are grouped and described in terms of method in the following paragraphs.

Concept Verification
In many cases, design concepts needed to be verified before being implemented in the design. For the sake of fluent reading, those tests and outcomes were all described previously in section 4. Design considerations.

Communication
Functions relating to communication are unique in the context of testing. Unlike other parts of the developed software these functions are purely soft with regards to input and output allowing them to be SIL tested in structured unit tests, as exemplified in table 9.

Test	Input	Expected outcome	Outcome
1	Some input 1	Expected output 1	Some Output
2	Some input 2	Expected output 2	Some output
.	.	.	.
.	.	.	.

Table 9: Example unit tests

Development of communicational software concerned both the transmitting and receiving side, resulting in high control and understanding of the data which greatly simplified the composition of realistic stimuli. Communicational functional tests were however also iterated through PIL and HIL tests:

- Transmitting and receiving strings between a PC and the Arduino nano and verifying expected outcomes (PIL)

Actuation
A bulk of the developed software comprised hardware-related functionality, activities such as motor driving, valve actuating and sensor reading naming a few. SIL is intuitively not suitable for register level (processor specific) code of this kind - instead of SIL testing, unit and functional tests under PIL and HIL were conducted. Expected signal outputs from the processor were verified using an oscilloscope. Expected hardware behavior was verified through serial printing, ocular inspection and an oscilloscope.

6.5 Robustness

Robustness is a key element in any system and therefor an important part to test.

LED and Resin
It became apparent once the resin had gone through the whole system a few times that the resin spreads on various parts of the complete design. Affected parts include the UV-LED:s, which naturally harden the surrounding resin when they are turned on. A test was designed to examine the impact of resin on the performance of the LED:s; how much resin could actually get stuck and hardened to the LED:s before the LED:s either brake or UV-light no longer gets through.

The test conducted was as simple as submerging an LED on a small PCB in resin, while having it connected to an active power supply. The subject was left submerged until the sphere of hardened resin no longer grew. The led was lit during the whole test and was tested again two days later. The execution of the test was documented and presented below in figure 66

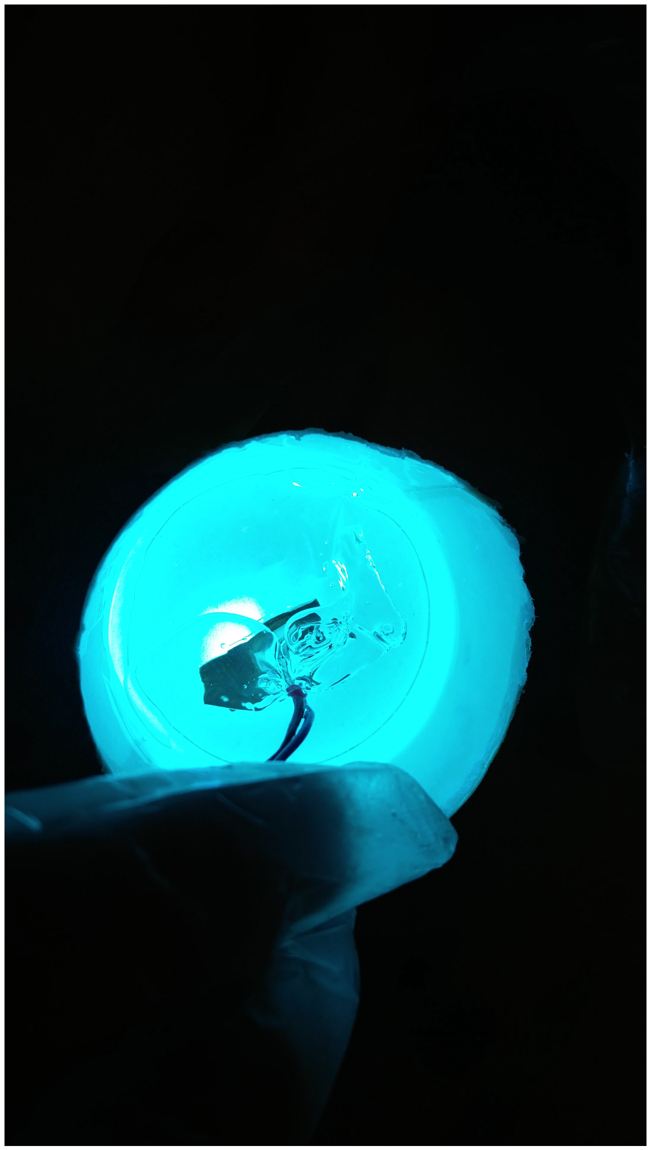

Figure 66: The Test for how the Led Handles Excess Resin

Printer head and Resin
Since the resin is toxic and slight acidic the parts that come in contact with it should be able to withstand such circumstances. The importance of this became apparent when resin spread through parts of the system that were not expected.

A basic test was conducted, were resin was fed through the system and excess resin inside the printer head was left to sit for approximately 10 hours. Parts were then inspected, more specifically in search of damage and erosion. The test was conducted with parts manufactured from two different plastics, PLA for test one and the formlabs resin for test two.

Printer head and UV-LEDs
Another thing that came to awareness was that the LED:s that exude UV-light as well as heat might impose threats to parts that are heat and UV-sensitive.

The test is conducted by having the whole printer head assembled and leaving on for a longer period of time, evaluating damages afterwards. An important note is that LED:s were run at higher power than at normally to grant extra intensity to the test.

Moving parts and Resin
As previously mentioned, the resin will, in the existing design, get in every nook and cranny, which poses the question; how are moving parts affected by resin potentially hardening in between moving surfaces? This prompted a test that is as simple as running the pump system for a short period of time, then running the LED:s for one minute and finally evaluating the maneuverability of the cutting mechanism.

7 Results

This section presents the outcomes of the tests described in section 6 Verification & Testing.

7.1 Material

The construction test conducted in section 6.1 Material resulted in one cube and one spiral, presented below in figure 67

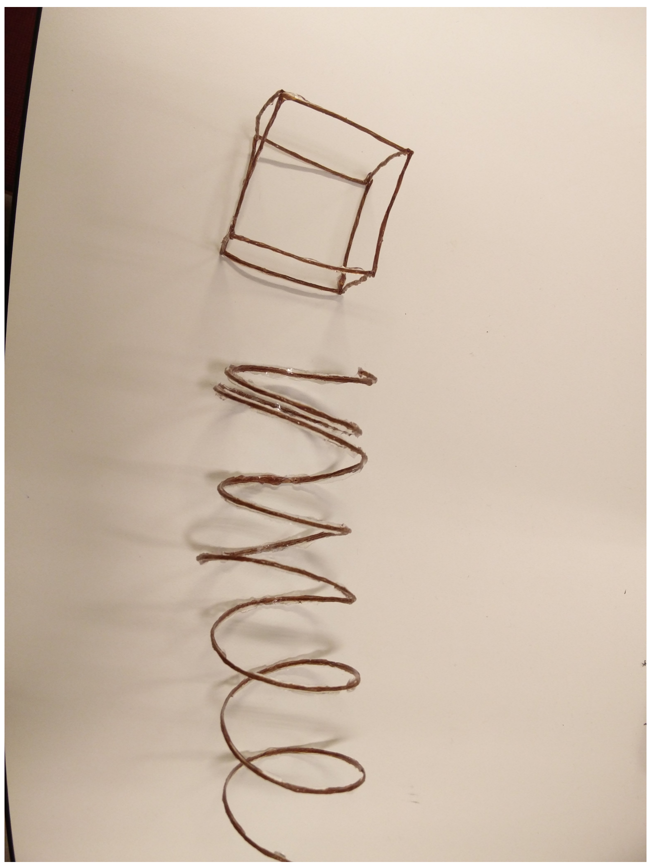

Figure 67: Cube and Spiral Made for Material Evaluation

Tensile tests were performed on three samples of different fiber-thread and resin compositions. The resulting tension-curves are presented below in Figure 68.

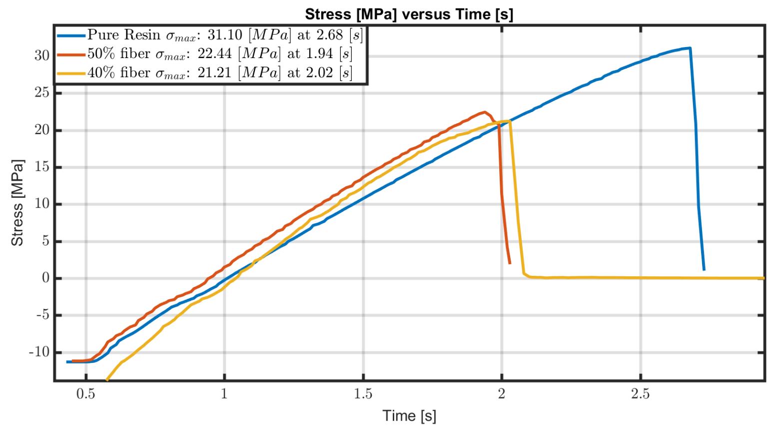

Figure 68: Applied tensile stress over time.

The same curves in terms of applied load is presented below in Figure 69.

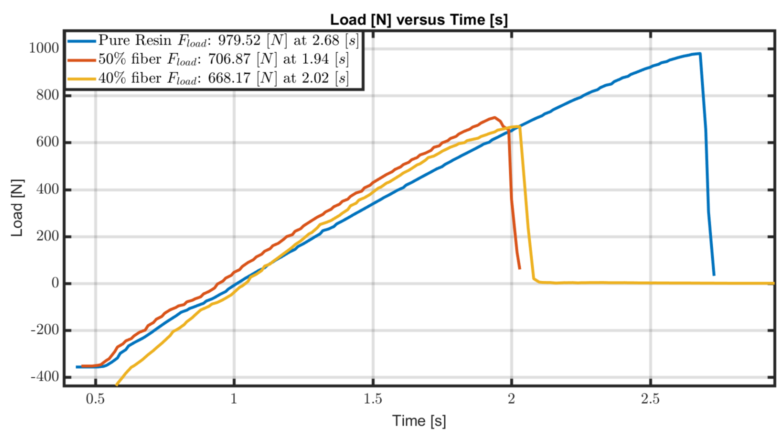

Figure 69: Load over time.

Sample extension and elongation data was extracted from the same tests and can be found below in Figure 70 and Figure 71.

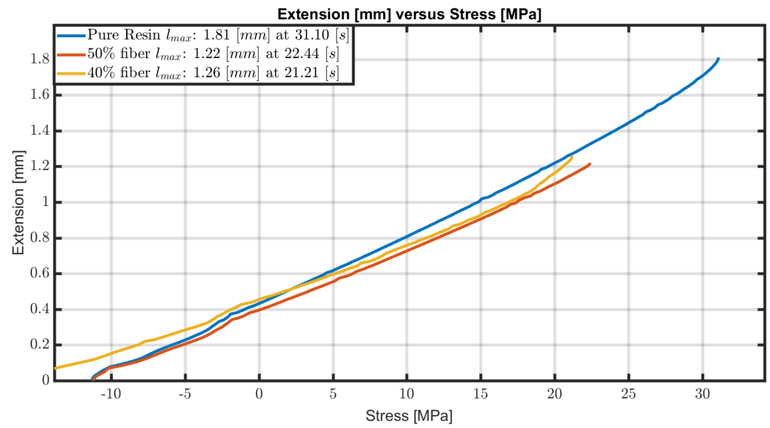

Figure 70: Sample extension as a function of stress.

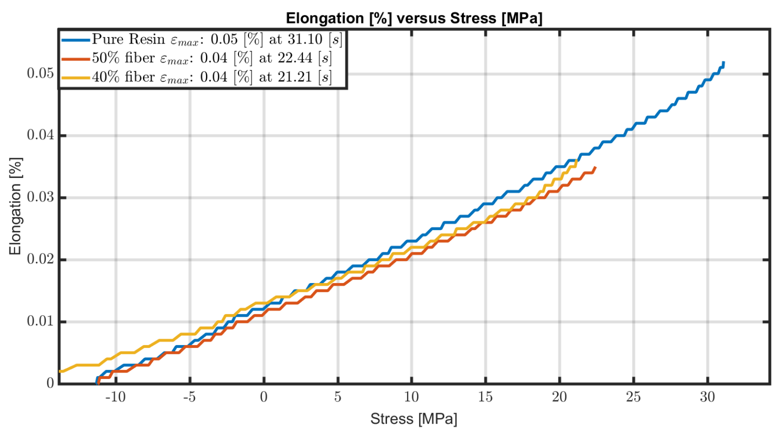

Figure 71: Sample elongation as a function of stress.

For reference, tensile tests were performed on ten samples of the cellulose thread. The results are shown in Figure 72 and 73 below.

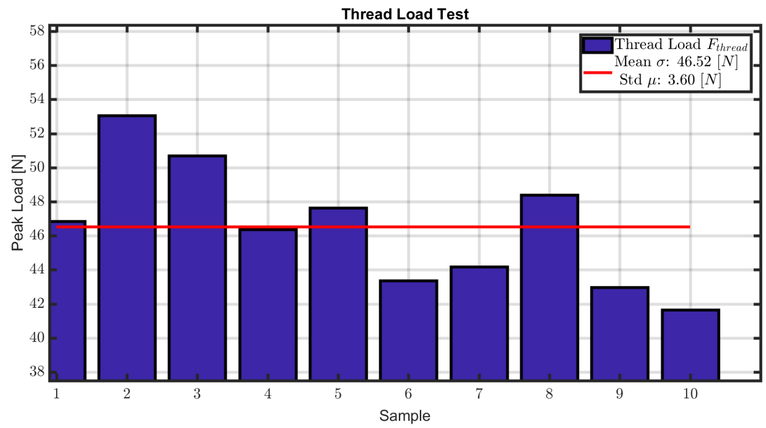

Figure 72: Tensile stress for ten samples of thread, along with the mean load over all samples

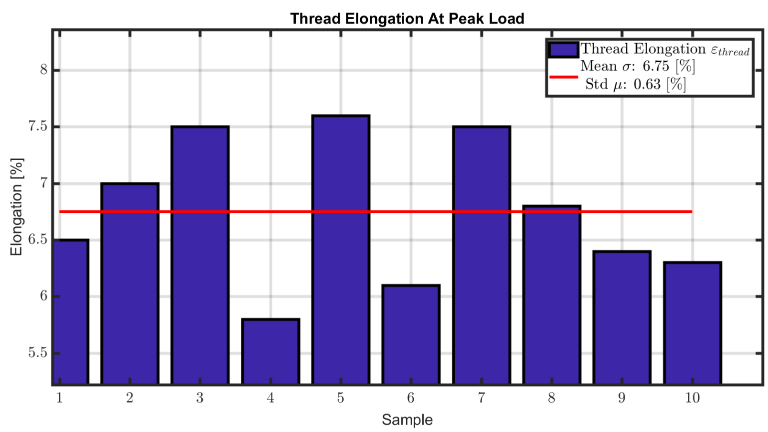

Figure 73: Percentual elongation at break for ten samples of thread, along with the mean elongation over all samples

7.2 Thread Feeding

The results from the test described in section 6.2 Thread Feeding are presented in table 10 below.

TEST	SPEED	FORCE	MEAN	ST. DEV.
1	HIGH	HIGH	-4.1%	11
2	HIGH	LOW	10.6%	18
3	LOW	HIGH	-4.9%	7
4	LOW	LOW	2.4%	10

Table 10: Results for thread feeding testing.

7.3 System Test

The printer managed to feed thread and pump resin as the robot was moving in a preprogrammed trajectory while the UV- hardening system was operating with the LEDs in on-state. This showed that system could print spatially in a 3-D space without having support material. The cutting mechanism could cut the thread in rare occasions, proving that the concept of cutting mechanism worked. Since the resin leaked out of the printer head in different sections, the resin hardened and clogged the hole in where the thread moved inside. The printer head could be easily mounted on an ABB IRB 120 robot with 4 screws.

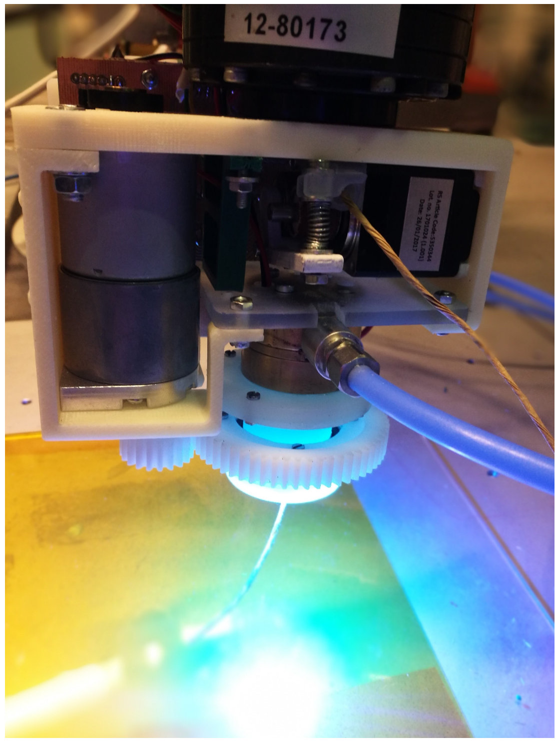

Figure 74: Test of the complete system. The printer is running the spiral software.

7.4 Verification

Requirements

In the tables below requirements are grouped and marked with Yes if they have been met, No if they have not been met and X if they have not been able to be verified.

Stakeholder Requirements	Met
1. The printer shall print without using a layer-by-layer method.	Yes
2. The printer shall print using no less than 50 percent cellulose fibers.	X
3. The printer shall not use support structures for printing objects.	Yes
4. The printer shall not produce toxic fumes that can affect the user's health.	X
5. The wood filament shall be cut when needed.	Yes
6. The printer head shall be modular.	Yes

Table 11: Evaluated Stakeholder Requirements.

User Requirements	Met
1. The printer head shall be mounted on a robotic arm.	Yes
2. The printer head shall be positioned with high accuracy.	Yes
3. The thread shall be evenly coated with coating material.	X
4. The thread shall be fed with high repeatability at various speeds.	No
5. The coated thread shall harden quickly.	Yes
6. The thread shall be cut with a high repeatability.	No

Table 12: Evaluated User Requirements.

Technical Requirements	Met
1. The total weight of the printer head shall not exceed 3 kg.	Yes
2. The repeatability of the nozzle position in the robots workspace shall be less than 10 % of the nozzle diameter.	Yes
3. The thread shall be fed within the speed interval 0-5 mm/s	Yes
4. The printer shall have an emergency stop.	No

Table 13: Evaluated Technical Requirements.

7.5 Robustness

Result regarding the tests conducted in section 6.5 Robustness will be presented here.

LED and Resin
The sphere of hardened resin around the LED expanded to a point were it was 14 mm in diameter, where the intensity of emitted UV-light was no longer capable of hardening more resin. However the LED did not stop functioning.

Printer Head and Resin
The documentation of the test 1 is presented in figure 75. The results is that the material used for test one crumbles after extended exposure to resin. Test 2 left only intact parts.

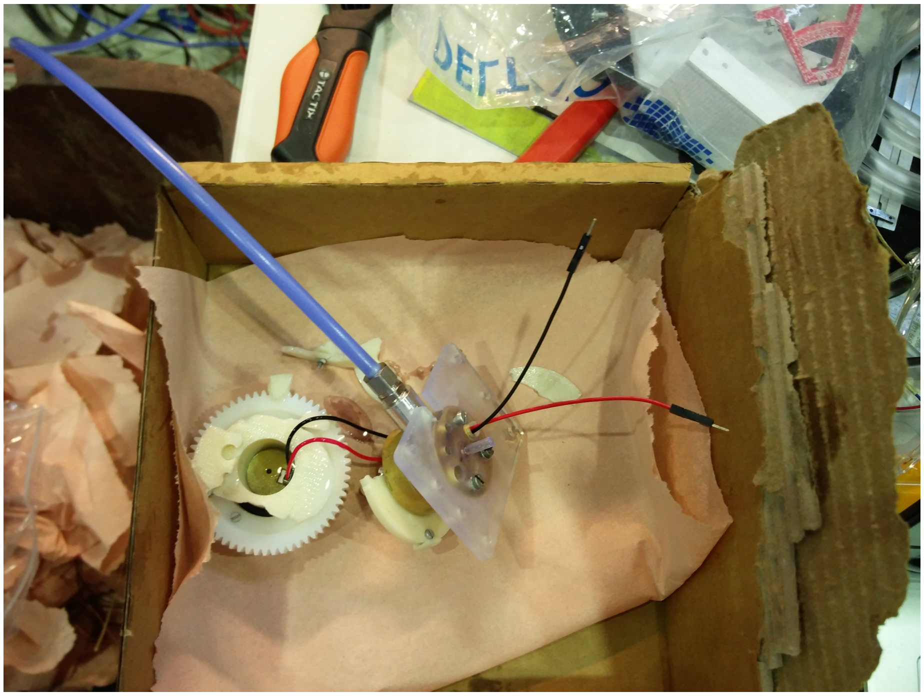

Figure 75: The impact of resin on the used material

Printer head and LED
Documentation from the test is shown in figure 76. As can be seen, the result is that both cracks and melting are visible. In addition it was found that LEDs de-soldered themselves due to the over-heating.

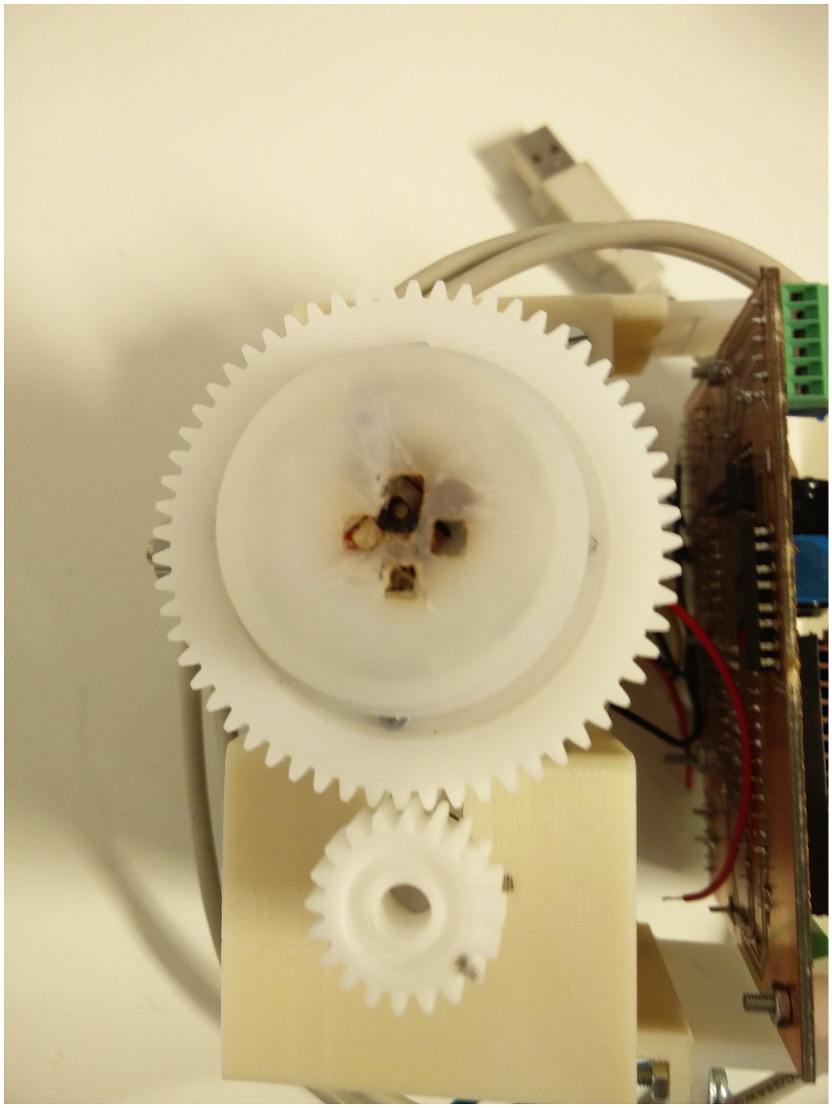

Figure 76: The Documentation of Testing the Impact of the Led on the Used Material

Moving Parts and Resin
The test revealed that, the cutter which does not move after the leak, hardens in between.

8 Discussion and Conclusion

This section discusses the obtained results and the conclusions that can be drawn from them. The requirements and design goals of the subsystem are also covered.

8.1 Requirements

Stakeholder requirements
In this paragraph, the different stakeholder requirements (refer to table 11) and whether these requirements were met or not are discussed. As explained in section 7.3 System Test functional tests were conducted with the printer. Referring to these tests, requirements 1, 3, 4 and 6 are deemed to be fulfilled.

Requirement 2 was not verified since the flow of resin could not be controlled properly. Due to unfortunate practicalities the pressure sensor for measuring pressure in the nozzle could not be implemented; the reason for this is that the a fitting that was ordered well in advance failed to be delivered. Therefore control of pressure was limited to the tank. Since the thread was coated with an unknown amount of resin one could not be sure of the ratio between wood and resin.

Requirement 4 was not verified since the equipment necessary to measure presence and toxicity of fumes could not be found within the limitations of the project (mainly time).

User requirements
In this paragraph the different user requirements (refer to table 12) and whether the requirements were met or not are discussed.

The first user requirement was met since the printer head could be easily attached and removed from the robot arm.

Requirement number 2 was also met due to the robot's accurate movement repeatability of 0.01mm [19].

Requirement 3 was not verified since the amount of resin that coated the thread varied during the printing process due to previously mentioned practicalities. The printer head leaked resin, flow could not be controlled and measuring it was not feasible.

Requirement 4 could not be met, see (6. Verification & Testing).

Requirement number 5 is ambiguous in the sense that it is formulated without a measurable variable. This was intentional since the thread had to be able to be fed at different speeds, which results in different hardening speeds. The thread hardened within seconds when using the UV-LED:s, which is considered to be 'fast enough'.

Requirement number 6 was not met due to the fact that the cutting mechanism only cut the thread occasionally when tested. The main reason for this malfunction is a slight space between the the cutting surfaces of the mechanism. Consequentially, instead of being severed, thread follows the blade and escapes into the small space due to the absence of counterforce.

A solution to this problem could be decreasing the space between the two cylinders and making sure that the right tolerances are taken into consideration in the manufacturing process. You might also add another blade, giving the appropriate counterforce.

Technical requirements
In this paragraph the different technical requirements (refer to table 13) and whether they were met or not are discussed.

The first requirement was met since the total weight of the printer head was 860g, as mentioned in (5.3Printer head.). In other words the weight limitation of 3 kg is far from exceeded.

The second requirement was also met due to the 0.01mm position repeatability of the IRB 120 robot [19].

Requirement number 3 was met since the printed thread, although the thread still had some flexibility, could stay relatively fixed. Requirement 4 was only partly met, since only one part of the system had an emergency button. The IRC 120 robot had such a button unlike the rest of the system. The only way to quickly shut down the other parts of the system was to turn of the power sources for them.

8.2 Material

The material compound, which constitutes a fundamental part of the project has been proven applicable in free form 3D-printing; it holds its own weight, hardens rapidly and can be fed through the printer head.

As for the strength of the material the results Material show that the resin is actually stronger without the thread in it. This is likely due to thread creating a cavity which makes the resin more brittle, something which the sher strength of the thread does not compensate for. The results concerning elasticity and elongation are even more confusing. The basic idea of a composite is to get a stiff and more elastic material but that is clearly not the case here.

However, studying figure 73 it can be concluded that the thread itself is not particularly elastic. Taking that into account whilst considering the fact that composites normally combine a stiff matrix with elastic reinforcements (reinforced concrete for example), the poor elasticity of the compound actually makes sense.

In the end it is a stiff, and durable material that is printable. The fact that the resin gets weaker from embedding fiber thread is a small concern in the bigger picture. The core of the project lies in the fiber thread which is actually reinforced by the resin.

8.3 Robustness

As seen in the earlier section 7.5 Robustness, the resin have prompted a few problems. The fact that it is so erosive was something that was not accounted for when designing the printer head. This meant that the material of choice had to be changed. Metal would have been preferred since it could withstand the erosive effect. Metal was initially though of, but excluded due to the numerous small parts of the printer head.

The resin has a tendency to flow into small cavities, such as the small space between two mated parts. If it is cured this causes problems with moving parts such as the cutter. This is a design flaw and is something that has to be solved for the system to work properly. The solution is to seal the printer head properly. This can be achieved using rubber gaskets. However, the cutter itself would still be in contact with the thread coated in uncured resin causing the same problem. A better alternative could be to cut the thread before coating. This in turn causes control issues as well as possible feeding issues and restricting printing to only print in sections longer than the distance from the cutter to the nozzle opening.

The led issues in melting and cracking from over-hardening would be solved by the previously mentioned solution of changing to metal. The LEDs seemed to be able to handle excess resin as long as the buildup of resin does not reach other parts. This could be solved by changing position or shield the LEDs so that the resin does not reach the LEDs. The fact that the LEDs de-soldered themselves after long runs is a major issue. This could be solved by cooling the LEDs and there is room for that in the existing design not just implemented due to shortage of time.

8.4 Thread feeding

The thread feeding is crucial in the printing process and has to be flawless. In order to validate the functionality of the thread feeder, tests were conducted, described in section 7.2 Thread Feeding. In the best configuration of the tests of the feeding mechanism there was 2.4% error. Some factors that affect this is slippage, thread getting stuck in the nozzle and human error. The reader should be aware that a positive mean error is something that should not happen since the movement of the feeding stepper motor is very precise.

Slippage is what happens when the friction between the thread and feeder is not enough and the feeder freewheels. Potential causes of slippage could be related to the force factor described in section 6.2 Thread Feeding. There is not enough force between the thread and feeder and therefore the friction is low, thus slippage occurs. If that factor is too high the inertia of the feeder could tear the thread apart which means the thread slips and does not move as intended. This is a tunable parameter that was intentionally built into the construction to allow slight modification.

The contact area between the thread and feeder is another potential cause of slippage. A larger contact means greater friction and vice versa. This problem can be addressed by selecting wheels of larger diameter. Another solution could be implementing a pulley system with several feeders which would decrease the need for friction due to the multiple contact areas of the feeders.

Slippage may occur if the thread is to heavy to feed which means there is a lot of friction in the way when the thread arrives to the feeder. This can be kept to a minimum if the inlet and tubing is smooth.

Thread getting stuck and curling is a problem that is difficult to deal with when pushing a non-stiff object from the rear through a tunnel. A possible solution to this problem could be if the whole nozzle was one solid piece, decreasing the friction where the thread moves. This could be an answer to why there is positive error. The thread might pile up while measuring and then when new test is conducted the excess thread comes out with that part.

Speed is a factor that can affect both previously mentioned factors as to why the thread does not feed as much as wanted. The speed increases the need for friction and thus the possibility of slippage also increases. The faster the thread moves, the more likely the thread gets stuck on an edge and then get stuck in the nozzle. Therefore a low speed should be preferred.

Human error is a likely factor as to why positive errors are seen since there are a lot of parts of the tests that a human is involved with, such as measuring and resetting for a new test. This does not make this any less relevant since all is done by the same person and correlation between the factors can be read through the results.

8.5 Summary

This section will summarize what has been concluded.

Several mechanical parts have been merged and integrated with software and electronics. The different parts were developed separately, and later tested together. Pros and cons were discussed and evaluated.

As mentioned earlier there is still room for improvement regarding robustness with- resin, feeding and UV-light. However, the main concept is proven to be working.

In addition, a point worth mentioning is that the design for assembly would be a good thing to implement as the existing model is hard to assemble and take apart. This has been a struggle when something needs to be evaluated, changed or just cleaned.

9 Future Work

This section presents the future work that is encouraged to proceed with in order to take 3D Printing in wood, further into the innovation process and eventually even using it industrially.

Automatic Path Generation
Everything was done manually during the project. A 3-D model had to be constructed by ourselves followed by creating a structure. The future work would include having an automatic path generation where in the program will take a 3-D model, build all the points that are needed and then feed it to the robot arm, creating parts of desired shape.

Improve Nozzle Shape
The bulkiness of the cutter mechanism limits the variety of objects that can be printed. For example, a hollow pyramid would cause the printer head to collide with the triangle when moving up and down. Improving the shape of the nozzle to have a longer and smaller tip, would allow the printer to operate in smaller spaces without collisions hence allowing a larger variety of objects to be printed.

Sustainable Resin
The resin that was used in the project work is not bio degradable, so ideally in the future, improved results can be obtained with the help of a sustainable resin.

Printer head
Difficulties were faced in having a compatible printer head. In future, the printer head can be more modular, meaning it should be easy to mount onto the robot. Choice of material for individual parts proved to be wrong, as it was observed how the the cutter began to crack (melt/dissolve) under the intense UV-light. A better material must be adopted in the future to avoid such issues. A future work can also be to include mirrors for the LEDs to direct the light towards the thread. In this way, one can ensure the LEDs are not exposed to the resin and doesn't melt as it did earlier.

Feeding Mechanism
The current feeding mechanism used in the project wasn't up to the mark and there were problems of thread curling. In order to reduce the risk of curling, a future alternative could be to include a flexible feeding mechanism where in the thread can be guided by a channel small enough to avoid curling.

Pump System
During the current project, there were problems in controlling the pressure from both sides of the flow pipe. This pressure could be better controlled if the tank could regulate pressure in both ways and can be implemented in the future.

Hence, one can ensure smooth flow from either side to know how much exact pressure flows through the pump system.

References

[1] Mathew Milnes. The mathematics of pumping water, 2014.

[2] Canalys. 3-d printing market grow us 162 billion, 2014. [Online; accessed 17-May-2017].

[3] Bio-Based News. Plastics in 3d printing markets: A ten-year opportunity forecast, 2014. [Online; accessed 15-May-2017].

[4] H. S. Carson M. Thiel C. J. Moore J. C.Borerro F. Galgani P. G. Ryan M. Eriksen, L. C. M. Lebreton and J. Reisser. Plastic pollution in the world's oceans: More than 5 trillion plastic pieces weighing over 250,000 tons afloat at sea. *PLoS ONE*, 9(12), 2014.

[5] Skogsindustrierna. *Skogsindustrin. en faktasamling. branschstatistik 2014*. 2014.

[6] Thoma Andreas Piškorec Luka Hack Norman Gramazio Fabio Kohler Matthias Helm Volker, Willmann Jan. Iridescence print: Robotically printed lightweight mesh structures. *3D Printing and Additive Manufacturing*, 2:117–122, 2015.

[7] Jaime Mata-Falcón Kathrin Dörfler Nitish Kumar Alexander Nikolas Walzer Konrad Graser Lex Reiter Heinz Richner Jonas Buchli Walter Kaufmann Robert J Flatt Fabio Gramazio Matthias Kohler Norman Hack, Timothy Wangler. Mesh mould: an on site, robotically fabricated, functional formwork. In *High Performance concrete and Concrete Innovation Conference*, 2017.

[8] Joris van Tubergen. Z-unlimited, 2017. [Online; accessed 18-May-2017].

[9] Apis-cor. Apis-cor 3d printer, 2017. [Online; accessed 18-May-2017].

[10] Joris Laarman-Tim Geurtjens Gijs van der Velden Stefanie Riegman Fabian Scheurer Luis Fraguada Mette Thomsen Areti Markopoulou Petr Novikov, Saša Jokić. Mataerial, 2017. [Online; accessed 18-May-2017].

[11] Giovanni Postiglione-Michele Tonizzo Andrea Mantelli, Gabriele Natale. Atropos, redefine manufacturing, 2016. [Online; accessed 18-May-2017].

[12] European Bioplastics. Bioplastics market data, 2016. [Online; accessed 17-May-2017].

[13] Luke Chilson. The difference between abs and pla for 3d printing, 2013. [Online; accessed 17-May-2017].

[14] David G. Rethwisch William D. Callister. *Fundamentals of Material Science and Engineering, 4th edition SI version.* John Wiley & Sons, Inc, 2012.

[15] Ferry P.W. Melchels. Celebrating three decades of stereolithography. *Virtual and Physical Prototyping*, 7(3):173–175, 2012.

[16] G.; Levi M.; Turri S.; Griffini G. Invernizzi, M.; Natale. Uv-assisted 3d printing of glass and carbon fiber-reinforced dual-cure polymer composites. *Materials*, 9(7):583, 2016.

[17] Gianmarco Griffini, Marta Invernizzi, Marinella Levi, Gabriele Natale, Giovanni Postiglione, and Stefano Turri. 3d-printable {CFR} polymer composites with dual-cure sequential {IPNs}. *Polymer*, 91:174 – 179, 2016.

[18] Brett G. Compton and Jennifer A. Lewis. 3d-printing of lightweight cellular composites. *Advanced Materials*, 26(34):5930–5935, 2014.

[19] ABB. Abb's smallest robot – for flexible and compact, 2017. [Online; accessed 02-Dec-2017].

[20] ABB. Industrial robot controller, 2017. [Online; accessed 02-Dec-2017].

[21] V&P Scientific INC. V&p scientific, 2010. [Online; accessed 18-Dec-2017].

[22] J.G. McGowan J.F. Manwell and A.L. Rogers. *Wind energy explained theory, design and application.* Chichester Wiley, 2002.

[23] Cagatay Basdogan. Discrete pid controller for use in robotics project 3, 2011.

[24] B.G. Lipták R. Siev, J.B. Arant. *Laminar Flowmeters of the Instrument Engineer's Handbook, Process Measurement and Analysis, Third Edition.* CRC Press, 2004.

[25] LLT FormLabs. Photoreactive resin for form 1, form 1+, form 2, 2016.

[26] Torkel Glad and Lennart Ljung. *Reglerteknik - Grundläggande teori.* Studentlitteratur, 2006.

[27] ABB. The toolbox for industrial robot users, 2017. [Online; accessed 02-Dec-2017].

[28] ABB. Operating manual, 2008. [Online; accessed 19-Dec-2017].

[29] Mark J. Anderson and Patrick J. Whitcomb. *Design of Experiments.* John Wiley and Sons, Inc., 2000.

Appendix

A. Project Costs

Total Project Cost	16147				
Budget Left	33854				

Article	Pris per unit excl VAT	Quantity	Total Cost	Ordered Date	Ordered By
Stepper Motor Feeder	586,05	1	586,05	05/10-2017	Simon Gärtner
UV glasses	27	4	108	05/10-2017	Simon Gärtner
Stepper Driver	763,77	2	1527,54	05/10-2017	Simon Gärtner
UV-LED	85,2	5	426	8/9-2017	Erik Landman
LED Driver	163,63	1	163,63	8/9-2017	Erik Landman
SPI/PROFIBUS Adapter	555	2	1110	19/9-2017	Simon Gärtner
Arduino Nano	171	2	342	05/10 - 2017	Simon Gärtner
mini USB to USB	69,9	2	139,8	05/10 - 2017	Simon Gärtner
pressure sensor	206,22	1	206,22	12/10-2017	philip Pulli
Stepper Motor Driver A4988	64,5	2	129	23/10-2017	Simon Gärtner
Safety Valve	109	1	338	30/10-2017	Sourjya Chowdhury
Thread Adaptor	46,9	1	462,2	31/10-2017	Sourjya Chowdhury
Wear Resistant Tubing	238,15	1	238,15	31/10-2017	Sourjya Chowdhury
Insert Fittings	120	2	240	31/10-2017	Sourjya Chowdhury
O-Ring	35	1	35	31/10-2017	Sourjya Chowdhury
D-Sub HD connector kit 44P	41,7	1	41,7	12/10 - 2017	Simon Ahlin Högfeldt
D-Sub plug kit 25P	22,8	1	22,8	12/10 - 2017	Simon Ahlin Högfeldt
Spiral cable wrap	39,92	1	39,92	06/10 - 2017	Simon Ahlin Högfeldt
Cable tie mount	27,92	1	27,92	06/10 - 2017	Simon Ahlin Högfeldt
PTFE tape	31,92	1	31,92	06/10 - 2017	Simon Ahlin Högfeldt
Black cable ties	39,92	1	39,92	06/10 - 2017	Simon Ahlin Högfeldt
optocouplers ILQ2-X009	23,18	4	92,72	30/10-2017	Erik Landman
dc/dc-converter rp15-2405sa	390,09	1	390,09	30/10-2017	Erik Landman
potentiometer 1kOhm	23,48	4	93,92	06/11-2017	Erik Landman
potentiometer 5kOhm	23,48	2	46,96	06/11-2017	Erik Landman
socket strip	44,256	10	442,56	06/11-2017	Erik Landman
Geared DC motor with Encoder	449	1	449	09/11-2017	Simon Gärtner
Aluminium Motor Mount	69	1	69	09/11-2017	Simon Gärtner
OP Amps	10		212	09/11-2017	Simon Gärtner
LED Power Supplies 0.7A LED DRVR REG 4.5-36Vin 2-35Vout	102	1	102	03/11-2017	Simon Gärtner
Isolated DC/DC Converters 15W DC/DC 1.6kV REG 18-36Vin 5Vout	390	1	390	03/11-2017	Simon Gärtner
Bipolar Transistors - BJT NPN Epitaxial Sil	7,64	5	38,2	03/11-2017	Simon Gärtner
Phoenix Contact COMBICON MPT Series 2.54mm Pitch Straight, PCB Terminal Block, Through Hole, 6 Way	26	10	260	03/11-2017	Simon Gärtner
McLennan Servo Supplies Bipolar Hybrid Stepper Motor 1.8°, 29Ncm, 2.3 A, 4 Wires	773	1	773	03/11-2017	Simon Gärtner
RS Pro Hybrid, Permanent Magnet Stepper Motor 0.9°, 0.22nm, 2.8 V, 1.33 A, 4 Wires	431	1	431	03/11-2017	Simon Gärtner
Vishay VLMU3500-405-060, VLMU3500 Series UV LED, 410nm 1250 mW @ 700 mAmW 60 °, 3-Pin Surface Mount package	78,29	4	313,16	03/11-2017	Simon Gärtner
PMA Nickel Plated Brass Cable Gland Locknut, M25 Thread	12	1	12	03/11-2017	Simon Gärtner
Deep Groove Ball Bearing W61805-2RS1 25mm I.D, 37mm O.D	506	1	506	03/11-2017	Simon Gärtner
Skalpell blades	24	4	96	14/11-2017	Todd Barker
Tomas cutting mechanism	700	2	1400		Todd Barker
Tomas pumping	700	4	2800		Philip Pulli
pressure sensor	206,22	1	206,22	6/11	Philip Pulli
Reely cogwheel SH1060HF	65	1	65	15/11-2017	Erik Landman
Reely cogwheel SH1020HF	36	1	36	15/11-2017	Erik Landman
DC/DC converters RPA30-2412SAW	332,95	2	665,9	16/11-2017	Erik Landman

Figure 77: The overall cost involved in completing the project.